



HAL
open science

**Terrigenous input off northern South America driven by
changes in Amazonian climate and the North Brazil
Current retroflection during the last 250 ka**

A. Govin, C. Chiessi, M. Zabel, A. Sawakuchi, D. Heslop, T. Hörner, Y.
Zhang, S. Mulitza

► **To cite this version:**

A. Govin, C. Chiessi, M. Zabel, A. Sawakuchi, D. Heslop, et al.. Terrigenous input off northern South America driven by changes in Amazonian climate and the North Brazil Current retroflection during the last 250 ka. *Climate of the Past*, 2014, 10 (2), pp.843-862. 10.5194/cp-10-843-2014 . hal-02180979

HAL Id: hal-02180979

<https://hal.science/hal-02180979>

Submitted on 11 Jul 2019

HAL is a multi-disciplinary open access archive for the deposit and dissemination of scientific research documents, whether they are published or not. The documents may come from teaching and research institutions in France or abroad, or from public or private research centers.

L'archive ouverte pluridisciplinaire **HAL**, est destinée au dépôt et à la diffusion de documents scientifiques de niveau recherche, publiés ou non, émanant des établissements d'enseignement et de recherche français ou étrangers, des laboratoires publics ou privés.



Terrigenous input off northern South America driven by changes in Amazonian climate and the North Brazil Current retroflexion during the last 250 ka

A. Govin¹, C. M. Chiessi², M. Zabel¹, A. O. Sawakuchi³, D. Heslop⁴, T. Hörner¹, Y. Zhang¹, and S. Mulitza¹

¹MARUM – Center for Marine Environmental Sciences, University of Bremen, Bremen, Germany

²School of Arts, Sciences and Humanities, University of São Paulo, São Paulo, Brazil

³Institute of Geosciences, Department of Sedimentary and Environmental Geology, University of São Paulo, São Paulo, Brazil

⁴Research School of Earth Sciences, Australian National University, Canberra, Australia

Correspondence to: A. Govin (aline.govin@uni-bremen.de)

Received: 12 September 2013 – Published in Clim. Past Discuss.: 25 October 2013

Revised: 7 March 2014 – Accepted: 12 March 2014 – Published: 28 April 2014

Abstract. We investigate changes in the delivery and oceanic transport of Amazon sediments related to terrestrial climate variations over the last 250 ka. We present high-resolution geochemical records from four marine sediment cores located between 5 and 12° N along the northern South American margin. The Amazon River is the sole source of terrigenous material for sites at 5 and 9° N, while the core at 12° N receives a mixture of Amazon and Orinoco detrital particles. Using an endmember unmixing model, we estimated the relative proportions of Amazon Andean material (“%-Andes”, at 5 and 9° N) and of Amazon material (“%-Amazon”, at 12° N) within the terrigenous fraction. The %-Andes and %-Amazon records exhibit significant precessional variations over the last 250 ka that are more pronounced during interglacials in comparison to glacial periods. High %-Andes values observed during periods of high austral summer insolation reflect the increased delivery of suspended sediments by Andean tributaries and enhanced Amazonian precipitation, in agreement with western Amazonian speleothem records. Increased Amazonian rainfall reflects the intensification of the South American monsoon in response to enhanced land–ocean thermal gradient and moisture convergence. However, low %-Amazon values obtained at 12° N during the same periods seem to contradict the increased delivery of Amazon sediments. We propose that reorganizations in surface ocean currents modulate the northwestward transport of Amazon material. In agreement with published records, the seasonal North Brazil Current retroflexion is intensified (or prolonged

in duration) during cold substages of the last 250 ka (which correspond to intervals of high DJF or low JJA insolation) and deflects eastward the Amazon sediment and freshwater plume.

1 Introduction

The Amazon River recently alternated between record floods in 2009 (Marengo et al., 2012) and 2012 (Satyamurty et al., 2013) and severe droughts in 2005 (Marengo et al., 2008) and 2010 (Lewis et al., 2011), both with severe socio-economic consequences. Observations over the last decades show signs of a changing water cycle in the eastern and southern regions of the Amazon Basin linked to deforestation, land use and climate change (e.g. Davidson et al., 2012). Although anthropogenic impacts do not yet seem to surpass the magnitude of natural hydrologic cycle variability (Davidson et al., 2012), model projections suggest that the Amazon Basin is nearing the transition into a disturbance-dominated regime (e.g. Malhi et al., 2008; Nobre and Borma, 2009). The lack of information on past natural precipitation variations, however, makes assessments of modern and future changes difficult and uncertain.

Lake sediment records provide a comprehensive view of South American tropical climate evolution since 20 ka (1 ka = 1000 years) (e.g. Behling, 2002; Sylvestre, 2009). The ongoing debate on moisture availability in Amazonia during

the last glacial maximum (LGM) relative to the late Holocene reflects the incomplete character of our knowledge about South American tropical precipitation (Sylvestre, 2009). Recent data compilations seem to agree on the existence of drier conditions in northernmost South American regions and wetter conditions in the tropical Andes during the LGM compared to the present (Sylvestre, 2009; Maslin et al., 2011). Complex glacial patterns are, however, observed in tropical lowland regions, in particular over the Amazon Basin (Sylvestre, 2009). A recent compilation indicates more arid Amazonian conditions during the LGM than today (Maslin et al., 2011). Nevertheless, precisely dated speleothem records challenge this scenario and suggest more subtle changes, with a wetter LGM in western Amazonia while drier conditions prevailed in easternmost Amazonia in comparison to the late Holocene (Cheng et al., 2013).

Few lake sediment records go beyond the last glacial period, when dating uncertainties are high (e.g. van der Hammen and Hooghiemstra, 2003; Ledru et al., 2009). Lacustrine sediments from Lake Titicaca (Baker et al., 2001b) and the Salar de Uyuni (Baker et al., 2001a) in the Bolivian Altiplano cover the last 50 ka and indicate wet conditions in the south tropical Andes during intervals of high austral summer insolation (i.e. ~ 25 – 36 and 38 – 50 ka). Over the last 370 ka, Lake Titicaca sediments reveal the largest changes in tropical Andean climate on glacial–interglacial timescales, with warm and dry (cold and wet) conditions during peak interglacial (glacial) periods, which suggest the effect of global temperature changes on regional water balance (Fritz et al., 2007; Hanselman et al., 2011). This site also documents millennial-scale events during the last glacial period, with wet conditions occurring during cold Greenland stadials (Baker et al., 2001a; Fritz et al., 2010). Such orbital and millennial-scale changes in South American tropical climate are supported by recent high-resolution and well-dated speleothem records. Few speleothem records documenting South American tropical climate on orbital timescales indicate strong precessional variations with increased rainfall during intervals of high austral summer insolation (Cruz et al., 2005; Cheng et al., 2013). NE Brazilian speleothems suggest an east–west anti-phase in precipitation over the last 25 ka, with humid conditions prevailing over NE Brazil and dry conditions over other South American tropical regions during the mid-Holocene period of low austral summer insolation (Cruz et al., 2009; Prado et al., 2013a, b). Finally, a growing number of speleothems document positive precipitation anomalies over most of Brazil and the Amazon Basin during Heinrich stadials due to increased moisture advection and southward migration of the intertropical convergence zone (ITCZ) induced by strong North Atlantic cooling (Wang et al., 2004; Kanner et al., 2012; Mosblech et al., 2012). Because factors other than rainfall intensity (e.g. source of moisture) can influence the oxygen isotopic composition ($\delta^{18}\text{O}$) of speleothems, the interpretation of these records in terms of past South American tropical precipitation changes

is, however, not straightforward (e.g. Cruz et al., 2005; Mosblech et al., 2012).

Marine sediments from continental margins have the potential to trace past changes in continental climate by recording variations in terrigenous input. In contrast to terrestrial archives, they have the advantage of integrating climate variability on a basinwide scale (Harris and Mix, 1999). Existing marine records show decreased input of terrigenous material in the Cariaco Basin (Peterson et al., 2000) and increased input off NE Brazil (Arz et al., 1999; Jaeschke et al., 2007) during Heinrich stadials. These results suggest dry and wet anomalies in northern South America and NE Brazil, respectively, hence supporting a southerly ITCZ position during periods of reduction in the Atlantic meridional overturning circulation (e.g. Peterson et al., 2000; Jaeschke et al., 2007). On longer timescales, glacial–interglacial changes in fluvial detrital inputs have been reconstructed in the Cariaco Basin for the last 580 ka (Yarincik et al., 2000) and in the western tropical Atlantic for the last 380 ka (e.g. Rühlemann et al., 2001; Bleil and Dobeneck, 2004) and 900 ka (Harris and Mix, 1999). Although changes in terrigenous supply seem to mirror sea level and insolation variations (Harris and Mix, 1999; Yarincik et al., 2000; Rühlemann et al., 2001), the existing records lack sufficient resolution to determine the climate mechanisms controlling them. Overall, a lack of high-resolution records that document the evolution of Amazon rainfall beyond the last glacial period impinges strongly on our understanding of Amazon natural variability.

To investigate the mechanisms driving orbital changes in South American tropical climate and terrigenous delivery, we present high-resolution geochemical records from four marine sediment cores located along the northern South American margin between 5° and 12° N. Sedimentary elemental composition enables the fluvial provenance of detrital material delivered to the core site to be traced, and past climate changes over the source regions to be reconstructed. We show the existence of strong precessional variations over the Amazon Basin during the last ~ 250 ka, with increased delivery of Andean material during periods of high austral summer insolation. Surface ocean currents then modulate the transport of Amazon material towards the Caribbean Sea. We show evidence that supports the proposed intensification of the North Brazil Current (NBC) retroflexion and associated oceanward deflection of Amazon material during cold substages of the last 250 ka (which correspond to periods of high austral summer insolation).

2 Regional setting

Modern precipitation in northern South America exhibits strong seasonal patterns (Fig. 1). North of the equator (e.g. over the Orinoco Basin), rainfall changes respond to the seasonal migrations of the ITCZ (e.g. Warne et al., 2002; Grimm, 2011). The wet and dry seasons occur during boreal

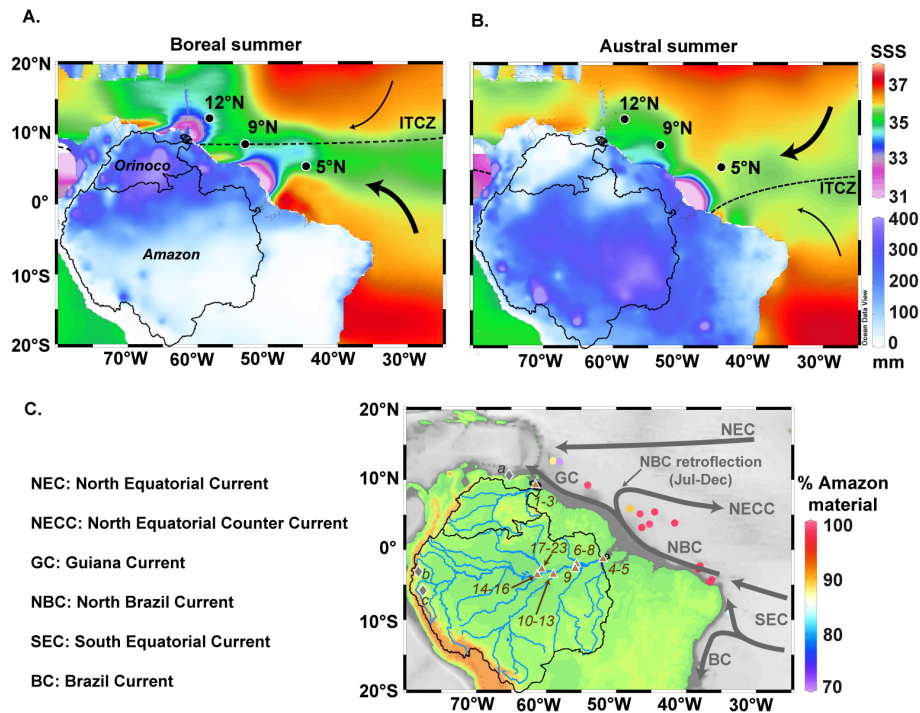


Fig. 1. Regional setting. Mean 1950–1999 terrestrial precipitation from the University of Delaware (<http://climate.geog.udel.edu/~climate/>) and mean sea surface salinity (SSS) from the World Ocean Atlas 2009 (Antonov et al., 2010) for (A) boreal summer (June–August for precipitation, September for SSS) and (B) austral summer (December–February for precipitation, March for SSS). The characteristic position of the intertropical convergence zone (ITCZ), and Orinoco and Amazon watersheds are shown. Black arrows illustrate the strength of the SE (strong in boreal summer, in A) and NE (strong in austral summer, in B) trade winds. Black dots mark the location of the studied sediment cores: GeoB3938-1 at 12° N, GeoB7010-2/GeoB7011-1 at 9° N and GeoB4411-2 at 5° N (Table 1). (C) Topography and bathymetry map. The main surface ocean currents are shown (Rühlmann et al., 2001). Coloured dots show the proportion of Amazon material within the terrigenous fraction (see Sect. 3.5) in surface sediment samples (Govin et al., 2012). Brown triangles show the position of river suspended samples used to define the elemental composition of endmembers (numbers refer to Table S3 in the Supplement). Grey diamonds show the location of published records: (a) Cariaco Basin (Peterson et al., 2000), (b) Santiago cave (Mosblech et al., 2012), (c) Cueva del Diamante cave (Cheng et al., 2013). Botuverá cave (Cruz et al., 2005) is located further to the south (27° S).

summer (mainly June–July–August, JJA) and austral summer (December–January–February, DJF), when the ITCZ has northern and southern positions, respectively (Fig. 1). Precipitation over most of the Amazon Basin is connected to the South American monsoon system (Grimm et al., 2005; Vera et al., 2006). During austral summer (DJF), strong heating over central South America enhances the northeast trade winds that lead to increased moisture levels onto the continent, hence causing intense precipitation over the Amazon Basin (Fig. 1) (e.g. Grimm et al., 2005). Heavy precipitation in northern South America is responsible for the high water discharge of the Amazon River ($6300 \text{ km}^3 \text{ a}^{-1}$), and to a lesser extent, the Orinoco River ($1100 \text{ km}^3 \text{ a}^{-1}$) (e.g. Meade, 1996; Peucker-Ehrenbrink, 2009). Due to the strong rainfall seasonality, peak water discharge, however, occurs during different seasons: May–July for the Amazon River (Meade et al., 1985) and August–September for the Orinoco River (Meade et al., 1990; Warne et al., 2002). The maximum in sediment discharge occurs mainly during the rising flood

discharge, that is, in February–April for the Amazon River and May–July for the Orinoco River (Meade et al., 1985, 1990; Warne et al., 2002).

The freshwater discharge of both rivers has a clear impact on the salinity of surface waters off northern South America (Fig. 1) (e.g. Hu et al., 2004). The Orinoco freshwater plume induces an anomaly of low sea surface salinity (SSS) that propagates into the Caribbean Sea, mainly during the peak discharge in boreal summer (Fig. 1a) (e.g. Müller-Karger et al., 1989). The NBC carries northwestward most of Amazon freshwater between January and June (Fig. 1b). Between July and December, part of the Amazon plume is deflected eastward by the NBC retroflection towards the North Equatorial Counter Current (Fig. 1a) (e.g. Müller-Karger et al., 1988; Lentz, 1995). Historical salinity data indicate that up to 70 % of Amazon freshwater is transported eastward when the NBC retroflection is fully established between August and October (Lentz, 1995).

Table 1. Marine sediment cores included in this study

Cruise	Core	Latitude	Longitude	Water depth (m)	References
M38/2	GeoB4411-2	5.43	−44.50	3295	Bleil and cruise participants (1998); Hörner (2012); this study
M49/4	GeoB7010-2	8.57	−53.21	2549	Fischer and cruise participants (2002); Kuhr (2011); this study
M49/4	GeoB7011-1	8.52	−53.25	1910	Fischer and cruise participants (2002); this study
M34/4	GeoB3938-1	12.26	−58.33	1972	Fischer and cruise participants (1996); Ahrens (2011); Schlünz et al. (2000); this study
	MD95-2042	37.80	−10.17	3146	Shackleton et al. (2000, 2002)

3 Material and methods

3.1 Sediment cores

We investigate four marine sediment cores located at 5° N (Ceara Rise, GeoB4411-2), 9° N (Demerara Plateau, GeoB7010-2 and GeoB7011-1) and 12° N (off Barbados, GeoB3938-1) (Table 1, Fig. 1). At 9° N, we combined two cores from proximal locations (Table 1) to obtain continuous records for the last 150 ka. The cores at 9 and 12° N are located along the pathway of the NBC and Guiana Current, while the site at 5° N is mostly under the seasonal influence of the NBC retroflection (Fig. 1). All cores receive terrigenous material delivered by the Amazon River, as observed in western equatorial Atlantic sediments (e.g. Zabel et al., 1999; Govin et al., 2012). The site at 12° N receives additional input from the Orinoco River (Schlünz et al., 2000). Hence, the cores are suitably located to trace past changes in Amazon and Orinoco terrigenous input, and in the strength of the NBC retroflection.

With water depth ranging between 1900 and 3300 m (Table 1), all core locations presently lie in North Atlantic deep waters (NADW). The sites are located above the modern and glacial positions of the calcite lysocline (Volbers and Henrich, 2004). Thus, calcite dissolution will have a very limited effect on the geochemical composition of the sediment. Past changes in aragonite dissolution may have an influence on cores GeoB7011-1 (1910 m), GeoB3938-1 (1972 m) and GeoB7010-2 (2549 m) that are located above or close to the modern lower aragonite lysocline (~2500 m, Gerhardt and Henrich, 2001) (see Sect. 5.1). Negligible aragonite content is expected in core GeoB4411-2 (3295 m) located well below the modern aragonite lysocline.

3.2 Foraminiferal stable isotopes

Stable isotopic records measured on the benthic foraminiferal species *Cibicides wuellerstorfi* were available

for core GeoB3938-1 (Schlünz et al., 2000). For the sites at 9° N, we produced benthic oxygen ($\delta^{18}\text{O}$) and carbon ($\delta^{13}\text{C}$) isotopic records every 2.5 cm in core GeoB7010-2 (5 cm in core GeoB7011-1) based on 1–8 specimens of *Cibicides wuellerstorfi* or *Uvigerina peregrina* picked from the sieved size fraction > 150 μm . In core GeoB4411-2, we picked 1–8 individuals of *Cibicides wuellerstorfi*, *Cibicides robertsonianus*, *Uvigerina* sp. or *Melonis* sp. (also from the sieved fraction > 150 μm) every 2 to 5 cm to produce a composite benthic $\delta^{18}\text{O}$ record. Analyses were performed at MARUM – Center for Marine Environmental Sciences, University of Bremen, with a Finnigan MAT 252 mass spectrometer coupled to an automatic carbonate preparation device. The working gas standard was calibrated against Vienna PDB (VPDB) using the National Bureau of Standards 18, 19 and 20 standards. The mean external reproducibility (1σ) of carbonate standards is better than 0.07 ‰. Classical correction factors were applied to the oxygen isotopic compositions of *Cibicides* sp. (+0.64 ‰, Shackleton and Opdyke, 1973) and *Melonis* sp. (+0.35 ‰, Shackleton et al., 1984) to meet *Uvigerina* $\delta^{18}\text{O}$ values and produce composite benthic $\delta^{18}\text{O}$ records.

3.3 Age models

3.3.1 Reference core MD95-2042

Following the approach of Shackleton et al. (2000), we revised the chronology of core MD95-2042 using the most recent AICC2012 ice core chronology (Bazin et al., 2013; Veres et al., 2013). This was performed in three steps. (1) The MD95-2042 planktic $\delta^{18}\text{O}$ record was correlated to NGRIP $\delta^{18}\text{O}$ record for the last 120 ka (Veres et al., 2013). Tie points were defined at the midpoint of abrupt temperature increases (as indicated by both proxies) associated with Dansgaard–Oeschger (D/O) events (Fig. 2). (2) Because abrupt warming events occurred simultaneously with increases in methane

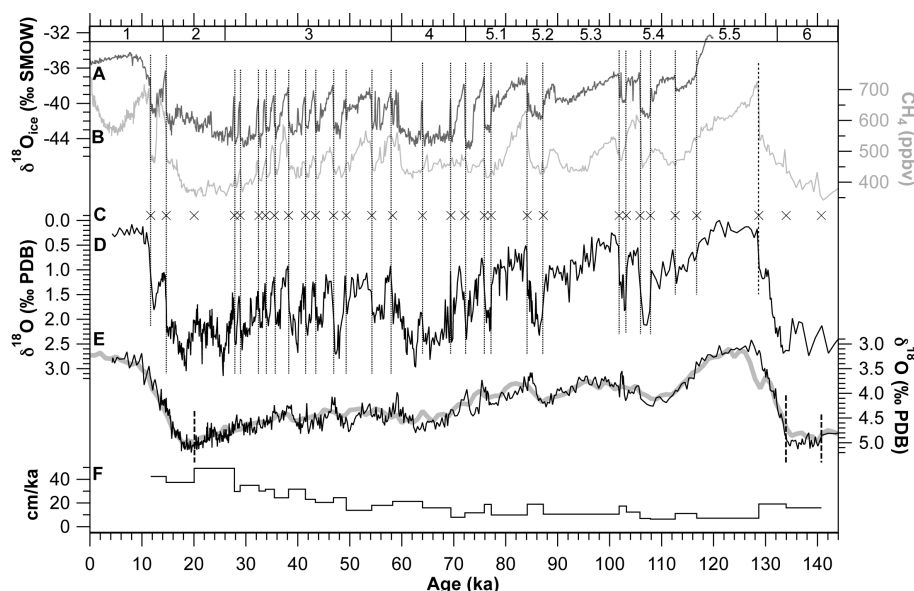


Fig. 2. Revised age model of reference core MD95-2042. **(A)** NGRIP ice $\delta^{18}\text{O}$ record on the AICC2012 timescale (Bazin et al., 2013; Veres et al., 2013). **(B)** EPICA Dome C (EDC) methane record (Loulergue et al., 2008) on the AICC2012 timescale (Bazin et al., 2013; Veres et al., 2013). **(C)** Defined tie points (crosses) in core MD95-2042. **(D)** Planktic foraminiferal $\delta^{18}\text{O}$ record from core MD95-2042 (Shackleton et al., 2000, 2002). **(E.)** Benthic foraminiferal $\delta^{18}\text{O}$ record from core MD95-2042 (Shackleton et al., 2000; Shackleton et al., 2002) in comparison to the benthic $\delta^{18}\text{O}$ stack (thick grey line) of Lisiecki and Raymo (2005). **(F)** Sedimentation rate variations in core MD95-2042. The vertical lines highlight the correlation points between MD95-2042 planktic $\delta^{18}\text{O}$ and NGRIP ice $\delta^{18}\text{O}$ records (dotted lines in **A–D**), MD95-2042 planktic $\delta^{18}\text{O}$ and EDC methane records (dashed line at 129 ka in **B–D**), and MD95-2042 and Lisiecki and Raymo (2005) benthic $\delta^{18}\text{O}$ records (thick dashed lines at 20, 134 and 141 ka in **E**). Marine isotope stages are indicated at the top of **(A)**.

(e.g. Chappellaz et al., 1993; Huber et al., 2006), we directly tuned the marine planktic $\delta^{18}\text{O}$ record to the abrupt Antarctic methane increase at the beginning of the last interglacial period (~ 129 ka, Fig. 2). (3) The close agreement of benthic $\delta^{18}\text{O}$ variations from core MD95-2042 and the reference stack (LR04) of Lisiecki and Raymo (2005) led us to define three additional tie points between both records during periods when the correlation to ice cores lacked robustness (Fig. 2e). The AICC2012 and LR04 chronologies have been independently defined, which may lead to offsets of few thousand years between both timescales. Despite the close agreement between LR04 and MD95-2042 benthic $\delta^{18}\text{O}$ variations over the periods (129–28 ka and 12–0 ka) where AICC2012 is the sole reference timescale, using the additional LR04 reference chronology may enhance dating uncertainties during the 144–129 and 28–12 ka intervals (Fig. 2). With this revised chronology, the sedimentation rate varies between 7 and 50 cm ka^{-1} in core MD95-2042 (Fig. 2f). These variations mirror those reflected in the initial age model (Shackleton et al., 2000).

3.3.2 South American cores

The age model of cores GeoB7010-2 and GeoB3938-1 is based on 7 and 4 AMS- ^{14}C dates, respectively (see Table S1 in the Supplement for details). The chronology for the lower

part of both cores, as well as for cores GeoB7011-1 and GeoB4411-2, is derived from the synchronization of benthic $\delta^{18}\text{O}$ records to core MD95-2042 for the last 150 ka and the stack of Lisiecki and Raymo (2005) before 150 ka (Fig. 3). We also employed the benthic $\delta^{13}\text{C}$ records (not shown) to improve the stratigraphic age control of cores where *Cibicides* data are available. Core GeoB7010-2 exhibits the highest sedimentation rate between 5 and 11 cm ka^{-1} , while all other cores have lower values between 1 and 6 cm ka^{-1} (Fig. 3). Therefore, the combined cores GeoB7010/7011 provide high-resolution records for the last 150 ka, whereas cores GeoB4411-2 and GeoB3938-1 have relatively high-resolution coverage for the last ~ 250 ka (Fig. 3). The age uncertainty is low for the interval covered by ^{14}C dating (< 0.4 ka, except for the date at 46.6 ka in core GeoB7010-2, Table S1 in the Supplement). The age error is ~ 2 ka for the period of the last 150 ka based on benthic synchronization. Due to the lower resolution of the earlier benthic records, the age uncertainty increases to 4 ka (Lisiecki and Raymo, 2005) between 150 and 250 ka (Fig. 3).

3.4 Major element composition

Elemental compositions of the four cores were measured using a XRF Core Scanner II (AVAATECH serial no. 2) at MARUM, University of Bremen. The XRF scanner

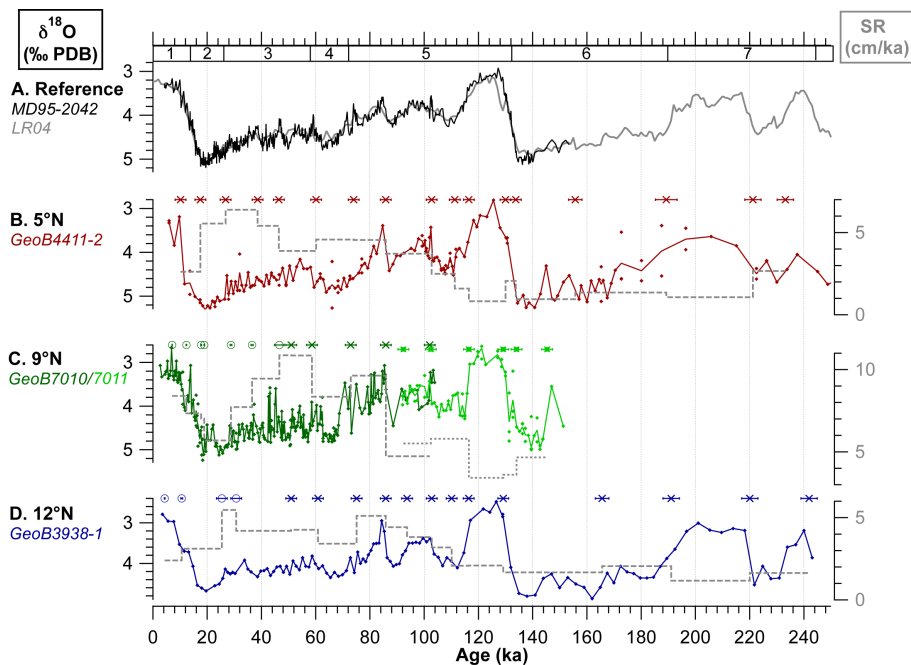


Fig. 3. Age models of the four studied sediment cores. **(A)** Reference records: benthic foraminiferal $\delta^{18}\text{O}$ records from the North Atlantic core MD95-2042 (Shackleton et al., 2000, 2002) (black line) and from the LR04 stack (Lisiecki and Raymo, 2005) (grey line). **(B)–(D)** Benthic $\delta^{18}\text{O}$ record (plain line, left y axis), sedimentation rate (SR) variations (grey dashed line, right y axis) and tie points (open circles for ^{14}C dates, crosses for tie points based on benthic synchronization, with 1σ errors) defined in cores **(B)** GeoB4411-2 (5° N, red), **(C)** GeoB7010-2 (9° N, dark green) and GeoB7011-1 (9° N, light green), and **(D)** GeoB3938-1 (12° N, blue). Marine isotope stages are indicated at the top of **(A)**.

measured major element intensities every 2 cm in cores GeoB7010-2 and GeoB7011-1, and every 1 cm in cores GeoB4411-2 and GeoB3938-1, by irradiating a surface of about 10 mm \times 12 mm for 20 s at 10 kV. In addition, we analyzed elemental concentrations on bulk sediment samples to calibrate the scanner intensities. We freeze-dried, powdered and homogenized between 30 and 45 samples per core (2–5 g of dry sediment). Major element concentrations were measured by energy dispersive polarization X-ray Fluorescence (EDP-XRF) spectroscopy (see Govin et al., 2012 for details). Using a log-ratio regression approach (Weltje and Tjallingii, 2008), we combined powdered measurements and scanner data to derive high-resolution calibrated proportions of six elements (Ca, Fe, Al, Si, Ti and K). The calibration used Ca as the common denominator element in the log-ratio regressions. The Fe/Ca log-ratios illustrate the quality of XRF calibrations (Fig. S1 in the Supplement).

3.5 Endmember unmixing analysis

Studies investigating South American palaeoclimate from the elemental composition of marine sediments are commonly based on the interpretation of specific ratios (e.g. Fe/Ca, K/Al, Ti/Al or Al/Si, Arz et al., 1998; Yarincik et al., 2000; Chiessi et al., 2010). However, such ratios depend on the geology, topography and climatic regimes of the

regions where terrigenous material originates, thus their interpretation within a climatic context is not straightforward (e.g. Govin et al., 2012). In northern South America, suspended sediments from lowland tributaries exhibit higher Al/Si, Fe/K and Al/K ratios than Andean tributaries (Table S2 in the Supplement), indicating high amount of heavily weathered clay minerals (e.g. kaolinite) in suspended sediments from tropical humid lowland regions (Guyot et al., 2007). In contrast, Amazon suspended material is characterized by a higher Al/Si ratio but lower Fe/K and Al/K ratios than the Orinoco River (Table S2 in the Supplement). Lower illite content and decreased K proportions in Orinoco suspended sediments (Eisma et al., 1978) are responsible for these compositional characteristics. Nevertheless, disentangling past changes in the contributions of Amazon and Orinoco material from specific elemental ratios is not a simple task.

In this study, we apply an endmember unmixing model (Mulitza et al., 2010; Collins et al., 2013) that facilitates the climatic interpretation of elemental records by using the integrated sediment composition and defining regional endmembers. In all cores, we determined past changes in the relative proportions of three endmembers: two terrigenous endmembers to disentangle the fluvial origin of terrigenous material and one marine endmember to account for the biogenic fraction of the sediment. To characterize the geochemical

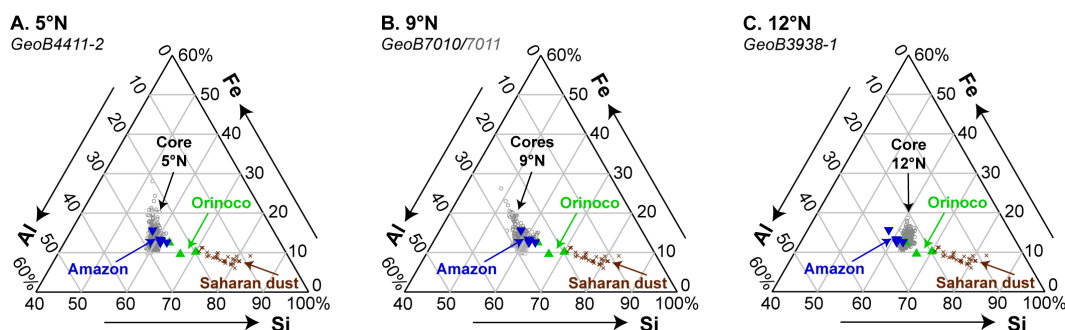


Fig. 4. Ternary diagrams highlighting the main sources of terrigenous material in the cores investigated in this study: (A) GeoB4411-2 (5° N), (B) GeoB7010/7011 (9° N) and (C) GeoB3938-1 (12° N). The relative Al, Fe and Si proportions are presented for all core samples (grey circles), Amazon (blue inverted triangles) and Orinoco (green triangles) river suspended material (see Table S3 in the Supplement for references) and Saharan dust (samples from Collins et al., 2013) for comparison.

composition of the terrigenous endmembers, we compiled existing and new geochemical data for the Amazon and Orinoco rivers, as well as for major Andean and lowland tributaries of the Amazon River (Table S3 in the Supplement). Amazon and Orinoco suspended material was used to define both terrigenous endmembers in the core at 12° N. Because the sites at 5 and 9° N almost exclusively receive sediment from the Amazon River (see Sect. 4.1), the relative proportions of Andean versus lowland Amazon material are estimated in these cores (Table S4 in the Supplement). In all cores, the marine endmember composition is set to fixed Si and Ca proportions defined from available carbonate and biogenic opal measurements at nearby sites (Table S4 in the Supplement). This assumption is supported by very small changes in western tropical Atlantic palaeo-productivity (Höll et al., 1999; Rühlemann et al., 1999) and low accumulation of biogenic opal in sediments (also on the Amazon continental shelf, DeMaster et al., 1983) (see footnote of Table S4 in the Supplement for details). To estimate uncertainties, we performed multiple iterations of the unmixing analysis. For each iteration, endmember compositions are held constant over time (see Sect. 5.2 for discussion of this assumption). The uncertainty on modern terrigenous endmember compositions is included by constructing spectra of endmember compositions via bootstrapping (Mulitza et al., 2010) and repeating the unmixing analysis 1000 times. Three different sets of Ca and Si proportions were used to include the uncertainty on the marine endmember composition (Table S4 in the Supplement). For %-Andes calculations in the 5 and 9° N cores, we also ran the unmixing analysis with three different sets of Amazon lowland elemental proportions to incorporate the uncertainty on Si concentrations in lowland samples (Table S3 in the Supplement). Therefore, the unmixing analysis was repeated 3000 times for the core at 12° N and 9000 times for the 5 and 9° N cores. The endmember proportions presented are mean values of all iterations. The proportion of one terrigenous endmember within the terrigenous fraction (“%-Amazon” or “%-Andes”) is the

median value of all iterations with non-parametric 95 % confidence intervals (2.5th and 97.5th percentiles).

4 Results

4.1 Elemental composition

In the cores at 5° and 12° N, Si is the most abundant element and accounts for ~45 % of the suite of six elements (Fig. S2 in the Supplement). Ca and Al represent around 20 % each, and Fe ~10 %. K and Ti are the least abundant elements (~5 and 1 %, respectively). In contrast, the cores at 9° N exhibit lower Ca contents (~10 %) and higher Si (~50 %) and Al (~23 %) proportions. Fe, K and Ti proportions are similar to those of the other two cores (Fig. S2 in the Supplement).

Comparing the relative proportions of the three most abundant detrital elements (Si, Al and Fe) to the modern composition of major terrigenous sources allows the primary provenance of the terrigenous material at the core sites to be identified (Fig. 4). The composition of the sediment cores matches that of South American fluvial particles (Fig. 4), which suggests a negligible input of North African dust relative to western tropical Atlantic riverine input. In addition, the geochemical composition of cores at 5 and 9° N closely matches that of Amazon suspended material (Fig. 4a–b), demonstrating that the Amazon River is the overwhelming source of terrigenous material at both sites. Finally, the sediment composition at 12° N is intermediate between that of Amazon and Orinoco suspended material (Fig. 4c), indicating that this site receives a mixture of Amazon and Orinoco detrital particles.

4.2 Endmember variations

Consistent with the described elemental proportions, the marine endmember accounts for ~20–25 % of the sediment at 5° and 12° N, and only ~10 % at 9° N (Fig. 5). The proportion of terrigenous material (relative to the marine biogenic endmember proportion) tends to decrease during past warm

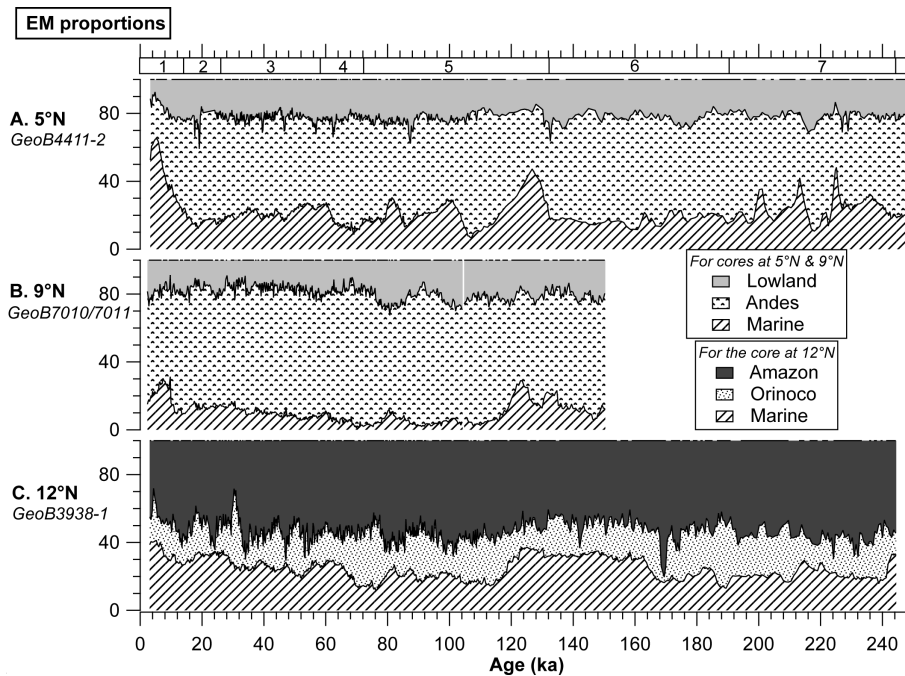


Fig. 5. Variations in the cumulative percentages of terrigenous and marine biogenic endmembers (EM) obtained in sites at (A) 5° N: GeoB4411-2, (B) 9° N: GeoB7010-2 (0–104 ka), GeoB7011-1 (105–150 ka) and (C) 12° N: GeoB3938-1 (see legend for filling patterns). The definition of endmembers is summarized in Table S4 in the Supplement. Marine isotope stages are indicated at the top of (A).

substages (marine isotope stages MIS 7, 5.5, 5.3, 5.1, 3 and 1) and increase during cold substages (Fig. 5). This feature is particularly visible in the 5 and 9° N cores and less clear at 12° N (Fig. 5). At 12° N, the Amazon and Orinoco endmembers on average account for ~55 % and 20 % of the sediment composition, respectively. Although the 12° N core is located relatively close to the mouth of the Orinoco (Fig. 1), Amazon material contributes ~70 % of the terrigenous fraction (Fig. 6). At 9° N, the Andean and lowland endmembers account for ~70 and 20 % of the total, respectively (Fig. 5), which implies that Andean material represents 77 % on average of the total terrigenous input (Fig. 6). At 5° N, the Andean and lowland endmembers account for ~60 and 20 % of the sediment (Fig. 5). Amazon material originating from the Andes hence contributes ~72 % on average of the terrigenous fraction at 9° N (Fig. 6).

The proportion of Andean material (hereafter called “%-Andes”) from sites at 5 and 9° N and the proportion of Amazon material (“%-Amazon”) from the core at 12° N exhibit variations on both millennial and orbital timescales over the last 250 ka (Fig. 6). This result is confirmed by spectral analysis (Fig. 7), which shows significant periodicities in the precession band (19–23 ka) and sub-orbital millennial timescales (Fig. 7). Given the age uncertainties and relatively low sedimentation rates (Fig. 3), we focus here on orbital variations and filtered the %-Andes and %-Amazon records to highlight changes in the precession band (Fig. 6). The sites at 5 and 9° N exhibit similar past %-Andes variations,

which generally follow changes in austral summer insolation, with high %-Andes values during periods of high DJF insolation (Fig. 6c–d). In contrast, the site at 12° N generally exhibits low %-Amazon values during intervals of high DJF insolation (Fig. 6e). %-Amazon precessional variations at 12° N hence appear to be in anti-phase to %-Andes changes recorded at 5 and 9° N (Fig. 6).

5 Discussion

5.1 Factors controlling terrigenous vs. marine biogenic proportions

Increases in terrigenous vs. marine biogenic proportions as observed in our study during past cold substages (Fig. 5) are common features of western tropical Atlantic sites (e.g. Arz et al., 1998; Harris and Mix, 1999; Zabel et al., 1999; Rühlemann et al., 2001). Several factors could influence the terrigenous vs. marine content of sediments and we successively evaluate the role played by global sea level changes, carbonate palaeoproductivity and carbonate dissolution.

Several studies suggest that past sea level variations influenced the amount and pathway of sediments delivered to the western tropical Atlantic (e.g. Schlünz et al., 2000; Rühlemann et al., 2001), in particular by the Amazon River (Milliman et al., 1975; Maslin et al., 2006). The discharge of Amazon sediments responds to a threshold mechanism driven by global sea level (Milliman et al., 1975). During

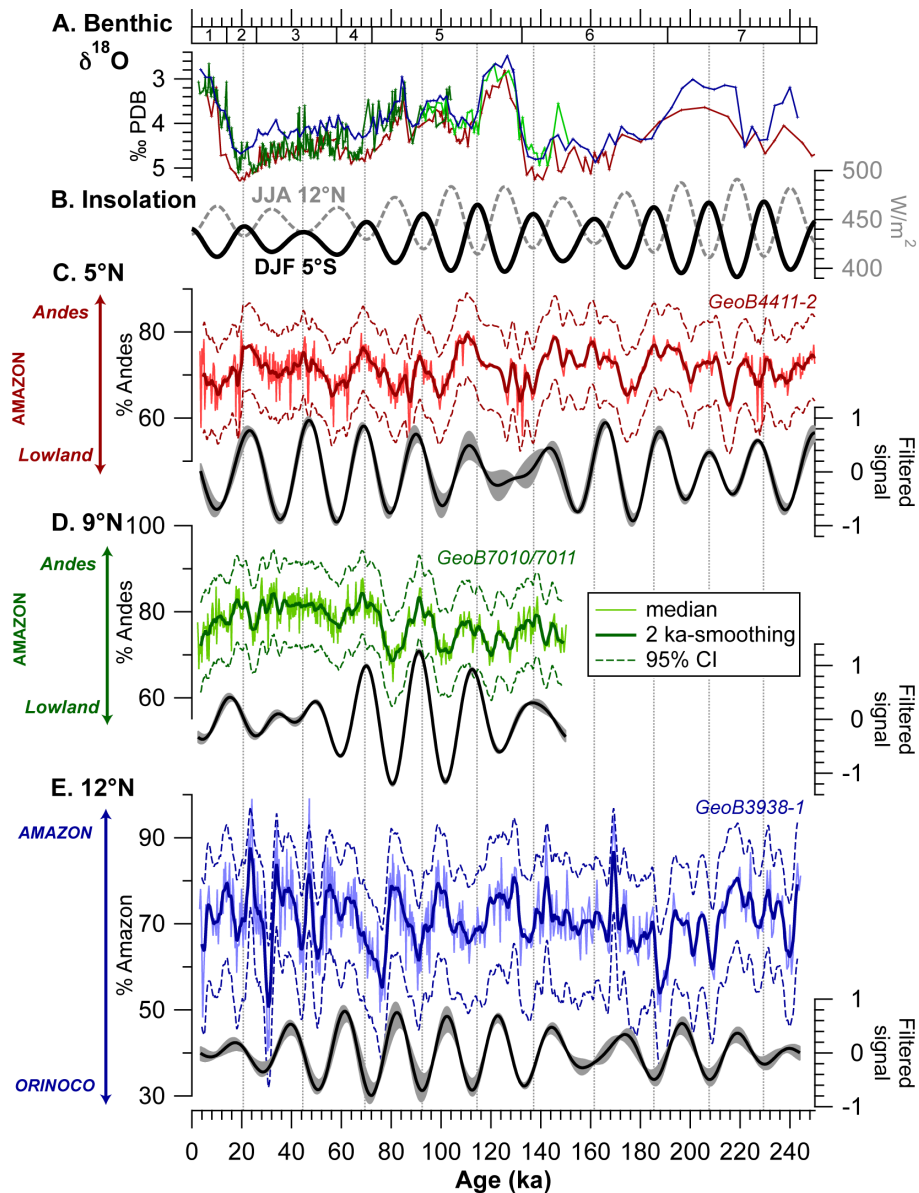


Fig. 6. (A) Benthic $\delta^{18}\text{O}$ records from cores GeoB4411-2 (red), GeoB7010/7011 (green) and GeoB3938-1 (blue). (B) December-January-February (DJF, black line) and June-July-August (JJA, dashed grey line) insolation curves (Laskar et al., 2004). (C)–(E) Percentages of Andean material (%-Andes in C and D) and Amazon material (%-Amazon 1 in E) within the terrigenous fraction (left y axes). Median values (light line = all data; thick line = 2 ka-smoothed data after resampling every 0.25 ka) and non-parametric 95 % confidence intervals (CI, 2.5th and 97.5th percentiles, dashed line = 2 ka-smoothed data) are presented. Records bandpass filtered in the 0.035–0.055 ka^{-1} frequency interval (periodicities of ~ 18 –28 ka) are shown on the right y axes. The black line and grey envelope represent the median and 95 % confidence interval (2.5th and 97.5th percentiles) of all filtered records, respectively. Grey vertical dotted lines highlight DJF (JJA) insolation maxima (minima). Marine isotope stages are indicated at the top of (A).

interglacial highstands, Amazon sediments are deposited by longshore currents along the continental shelf to the northwest of the river mouth. During glacial times when sea level falls 80–100 m below the present level, Amazon sediments are directly channelled down the continental slope (Milliman et al., 1975; Maslin et al., 2006). Increased glacial sediment delivery to the deep sea led to sedimentation rates in the

Amazon Fan that were about 20 to 1000 times higher than during the Holocene (Milliman et al., 1975; Maslin et al., 2006). Therefore, sea level variations likely influenced the total amount of terrigenous material deposited at our core sites and explain the relative increases in terrigenous vs. marine biogenic endmember proportions observed during cold substages (Fig. 5).

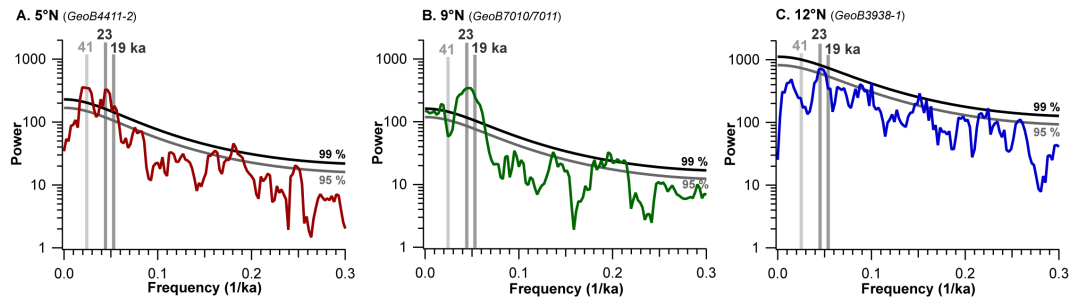


Fig. 7. Multitaper method (MTM) spectral analysis (Ghil et al., 2002) (number of tapers 3; bandwidth parameter 2) of detrended %-Andes records for sites at (A). 5° N: GeoB4411-2, (B) 9° N: GeoB7010/7011, and of the detrended %-Amazon record for the site at (C). 12° N: GeoB3938-1. 95 % (grey line) and 99 % (black line) significance levels are shown and the main statistically significant peaks (periods in ka) are indicated. Vertical bars highlight the position of the 1/41 (light grey), 1/23 and 1/19 ka⁻¹ (dark grey) frequencies.

Reconstructions of palaeoproductivity on Ceara Rise (close to our 5° N site) indicate low carbonate productivity over the 300 ka (as expected for this oligotrophic region), with slightly enhanced productivity values during past warm substages if compared to glacial intervals (Rühlemann et al., 1999). This result suggests that changes in carbonate productivity could contribute to the decreases in terrigenous vs. marine biogenic proportions observed during warm substages (i.e. MIS 7, 5.5, 5.3, 5.1, 3 and 1, see Sect. 4.2, Fig. 5). However, such small productivity variations are probably overprinted by the large deep-sea input of terrigenous material induced by lower glacial sea levels (Rühlemann et al., 2001).

Because all core sites are located above the modern and glacial calcite lysocline (Volbers and Henrich, 2004), calcite dissolution will have a very limited effect on the sediment's composition. In contrast, aragonite dissolution could affect the geochemical composition of three cores (1900–2550 m, Sect. 3.1) located above or close to the modern lower aragonite lysocline (~ 2500 m, Gerhardt and Henrich, 2001). Results from a NE Brazilian core from a similar water-depth range (2070 m) indicate aragonite contents ranging between 10 and 30 % of the total weight (~ 15 % on average) with increased bottom-water corrosiveness and aragonite dissolution during past cold substages (in response to deep-water changes, Gerhardt et al., 2000). Similarly, increased aragonite dissolution during glacial intervals could contribute to increases in terrigenous vs. marine biogenic proportions, as described here (Fig. 5). However, we suggest that large changes in sediment delivery induced by global sea level variations dominate the effect of carbonate dissolution and are the main driver of terrigenous vs. biogenic changes recorded in deep sediments.

5.2 Factors controlling the %-Andes and %-Amazon tracers

Unmixing the elemental composition of surface sediments (Govin et al., 2012) reveals very high %-Amazon values (> 98 % in most cases) in samples located between 3 and

9° N (Fig. 1c). Hence, Amazon material dominates the input of terrigenous particles along northern South America. This result agrees with the Amazon provenance of detrital material identified in cores at 5 and 9° N (Fig. 4) and in sediments from the equatorial western Atlantic (e.g. Zabel et al., 1999; Rühlemann et al., 2001). Surface sediments at 13° N exhibit high %-Amazon values (~ 78 % on average, Fig. 1c) that are within the range of past %-Amazon variations recorded in the sediment core at 12° N (Fig. 6e). These values indicate that both the Amazon and Orinoco rivers contribute to terrigenous inputs off Barbados (Schlünz et al., 2000). However, with a sediment discharge ten times higher than the Orinoco River (Meade, 1994), the Amazon River remains the major contributor of sediments deposited along the northern South American margin, even in the vicinity of the Orinoco delta (Warne et al., 2002). It explains the high proportion of Amazon material in sediments collected off Barbados (Figs. 1c and 6e), despite the proximity of the Orinoco River mouth. Thus, the endmember unmixing model produces %-Amazon values that are in agreement with the modern depositional environment of the western equatorial Atlantic.

Between 3° and 9° N where the Amazon River is the sole source of detrital sediments, the unmixing model produces %-Andes values around 72 and 77 % in the two studied sediment cores (Fig. 6c–d) as well as in surface sediments (not shown). The reason why %-Andes values are slightly higher at 9° N than at 5° N (Fig. 6) is unknown. Nevertheless, although slightly too low, such high proportions of Andean material in marine sediments reflect the large delivery (> 90 %) of suspended sediments by Andean tributaries within the Amazon Basin (Meade et al., 1985; Guyot et al., 2007). The endmember unmixing approach hence produces %-Andes values that agree with the modern provenance of Amazon terrigenous sediments. High precipitation, steep topography and lithology are responsible for intense erosion in the Andes and very large amounts of sediments delivered by Andean tributaries to the Amazon under modern times (Masek et al., 1994; Aalto et al., 2006). The amount of transported suspended sediments is an important criteria used to

classify Amazon tributaries into the three traditional categories (Sioli, 1984; Meade, 1994): white waters (very high suspended load, e.g. Madeira, Solimões Rivers), clear waters (relatively low suspended load, e.g. Tapajós River) and black waters (very low suspended load, e.g. Negro River). The small amplitude of %-Andes variations recorded at 5° and 9° N ($\pm 10\%$ around averaged values, Fig. 6) hence reflects the stability of this Amazon sedimentary system over the last 250 ka. Due to steep topography and intense erosion in the Andes, Andean tributaries remained the main source of Amazon sediments over the last 250 ka, while past Amazonian precipitation changes are likely responsible for the small amplitude of %-Andes variations (see Sect. 5.3). Storage of suspended sediments in Amazonian floodplains (Meade et al., 1985) could also minimize the amplitude of suspended load variations driven by precipitation changes.

Several factors could influence the past %-Amazon and %-Andes variations recorded in our western tropical Atlantic cores. Although the export of North African dust is increased during glacial times (Kohfeld and Harrison, 2001; Mahowald et al., 2006), we show that fluvial inputs remain the dominant sources of terrigenous material at the core sites over the last 250 ka (Fig. 4). Past changes in North African eolian input are thus unlikely to strongly affect the geochemical composition of western tropical Atlantic sediments (Zabel et al., 1999), that is, eolian input will play a minor role in driving past %-Amazon and %-Andes variations.

Sea level variations may have influenced the relative proportions of terrigenous material delivered by Amazon Andean and lowland tributaries (i.e. the %-Andes records). According to early sequence stratigraphy models, sea level decrease favours the incision of river valleys and increases the erosion and transfer of sediments to the ocean (Posamentier et al., 1988). However, the response of large river systems to Quaternary sea level changes is not straightforward and depends on many other variables (Blum et al., 2013). Draining soft sedimentary terrains, lowland rivers would be more sensitive to increased valley incision and erosion due to sea level drops than Andean tributaries (Blum et al., 2013). Therefore, a relative increase in sediment supply from lowland tributaries is expected during periods of sea level fall. The 5 and 9° N records exhibit increasing %-Andes values during the transitions between MIS 7–6, 5.5–5.4, 5.3–5.2, 5.1–4 and 3–2 (Fig. 6). This result indicates a relative decrease (increase) in sediment supply from lowland (Andean) tributaries during intervals of sea level fall of the last 250 ka and suggests that sea level variations do not primarily control the %-Andes records. In contrast, intermediate glacial sea levels appear to have modified the delivery pathway of Orinoco sediments to the core site at 12° N and allowed the accumulation of terrestrial organic matter (Schlünz et al., 2000). Our data do not reproduce the relationship between accumulation rate of total organic carbon and sea level observed by Schlünz et al. (2000) and we do not observe any relationship between sea level and %-Amazon in this core (Fig. S3 in the

Supplement). Major areas contributing to the runoff of Andean and lowland tributaries of the Amazon River are located thousands of kilometres away from the coast. The response of large rivers to shifts in erosion base level is thus slow and can reduce the effect of sea level changes on fluvial sediment supply to the ocean (Blum et al., 2013). Also, surface stabilization due to vegetation growth plays an important role for sediment erodibility and transport in tropical rivers (Tal and Paola, 2007; Nicholas, 2013). The effect of high frequency sea level changes on the sediment supply of large tropical rivers can be surpassed by climate events affecting runoff and vegetation cover. Altogether, although the influence of sea level variations cannot be completely excluded, we argue that sea level changes do not exert the primary control on our terrigenous records.

The mineralogy of the sediment controls its geochemical composition, as well as the grain size of detrital particles (Bloemsmas et al., 2012). Thus, elemental ratios can be highly related to grain-size variations (Mulitza et al., 2008; Bouchez et al., 2011), in response to mineralogical modifications induced by changes in weathering, sorting or mixing processes (Bloemsmas et al., 2012). Among the terrigenous elements considered here, Si and Ti are the most likely to be connected to grain-size changes. While Al, K and Fe are mainly associated with fine-grained clay particles in marine sediments (Biscaye, 1965; Yarincik et al., 2000), Si and Ti are associated with clay minerals but also with coarse quartz and rutile grains, respectively (Moore and Dennen, 1970; Schütz and Rahn, 1982). Because Ti accounts here for less than 1 % (Fig. S2 in the Supplement), grain-size sorting processes involving Ti will have a negligible imprint on the %-Andes and %-Amazon records. In contrast, Si accounts for almost half of the elemental composition (Fig. S2 in the Supplement). Si variations are mostly related to grain-size changes in environments rich in coarse quartz grains, in particular sediments receiving large amounts of wind-blown dust off North Africa (Bloemsmas et al., 2012). Located at great water-depths (> 1900 m) and far away from the continental shelf, the sediment cores considered here contain terrigenous material mainly in the clay fraction (Fischer and cruise participants, 1996, 2002; Bleil and cruise participants, 1998). In addition, because Al and K are both associated with fine-grained clay particles, the Al/K ratio is independent of grain-size sorting. Therefore, the highly similar variations exhibited by Al/Si and Al/K log ratios (Fig. S4 in the Supplement) indicate that sorting processes have a very limited signature in Si proportions in the studied cores, and hence on the %-Andes and %-Amazon records.

Bottom-water currents may transport clay minerals, hence modifying the composition of marine sediments (Petschick et al., 1996). However, it is very unlikely that bottom-water currents discriminate between the Andean and lowland material contained in suspended sediments delivered by the Amazon River. Hence, the %-Andes records obtained at 5 and 9° N (Fig. 6c–d) should not be affected by sediment transport

via changes in bottom-water currents. With a water depth of 1972 m, our core site at 12° N presently lies in the southward-flowing NADW. During cold substages, enhanced proportions of northward-flowing Antarctic bottom waters in the deep tropical Atlantic (Curry and Oppo, 1997) could have favoured transport of Amazon material to the core site. However, such cold intervals are characterized by decreased (increased) proportions of Amazon (Orinoco) material (Fig. 6e). Therefore, it is unlikely that bottom-water currents are responsible for orbital-scale %-Amazon variations recorded at 12° N. We thus rule out the possibility of a strong bottom current influence on the %-Andes and %-Amazon records.

In light of the arguments made above, we propose that the %-Andes and %-Amazon variations recorded in the western tropical Atlantic (Fig. 6) mainly reflect changes in South American fluvial input, that is, in the relative amount of Amazon Andean material at 5 and 9° N and of Amazon material at 12° N (see Sect. 5.4 for discussion on the influence of surface-water currents at 12° N).

5.3 Past changes in Amazonian precipitation

We now focus on the %-Andes records, which exhibit strong precessional variations (Fig. 6c–d). Despite the relatively large 95 % confidence intervals, precessional %-Andes variations are significant, as indicated by spectral analysis (Fig. 7) and filtered records (Fig. 6). The %-Andes confidence intervals are calculated as the 2.5th and 97.5th percentiles of 9000 bootstrap iterations. The composition of Andean and lowland endmembers slightly differs for every iteration, within the modern variability defined by available fluvial suspended data (Table S3 in the Supplement). This approach thus produces individual %-Andes records (not shown) characterized by highly similar variations but shifted towards lower or higher %-Andes values. It explains the robustness of precessional %-Andes changes at 5 and 9° N, despite the large 95 % confidence intervals (Fig. 6).

Despite small offsets probably related to absolute dating uncertainties, we generally observe high %-Andes values, that is, increased (decreased) proportions of Andean (lowland) material, during periods of high DJF insolation (Fig. 6c–d). This result agrees with the study by Harris and Mix (1999), which showed decreased sediment supply from Amazon lowland regions during low JJA (i.e. high DJF) insolation. We suggest that increased amounts of Andean vs. lowland material during periods of high austral summer insolation are related to enhanced precipitation over the Amazon Basin, in particular over Andean tributaries. This hypothesis is supported by the similarities between %-Andes and western Amazonian and southern Brazilian speleothem records (Fig. 8), which indicate strong coupling between the intensity of the South American monsoon and austral summer insolation variations over the last 250 ka (Cruz et al., 2005; Mosblech et al., 2012; Cheng et al., 2013). Lake sediments from the Bolivian Andes, which show alternating wet and dry

phases over the last 370 ka, with wet phases occurring during periods of high austral summer insolation (Baker et al., 2001a, b; Fritz et al., 2007; Gosling et al., 2008; Hanselman et al., 2011) further support our assumption.

By analogy with the modern austral summer situation in South America (Grimm et al., 2005), high DJF insolation increased the land–ocean temperature contrast by enhancing heating over central South America. Strengthened NE trade winds transported an increased amount of moisture to the continent, which intensified the South American monsoon (Cruz et al., 2005) and increased Amazonian rainfall (Mosblech et al., 2012). Maslin et al. (2011) proposed that moisture availability over the Amazon Basin results from the combined effects of (1) precession-driven changes in the South American monsoon intensity (as described above) and (2) the position of both northern and southern boundaries of the ITCZ, which migrate according to the meridional thermal gradient of each hemisphere. We cannot disentangle these effects based on our %-Andes data, which integrate climatic changes over the entire Amazon Basin. However, periods of high DJF insolation are also intervals of low JJA insolation and correspond to cold substages of the last 250 ka (Fig. 6). We can hence draw a parallel between our observations during periods of high DJF insolation and the glacial situation proposed by Maslin et al. (2011). Enhanced meridional thermal gradients in both hemispheres during glacial times tend to shift the northern and southern boundaries of the ITCZ towards the equator (e.g. Chiang and Bitz, 2005). Therefore, the resulting latitudinal contraction of the South American rain belt and the intensification of the South American monsoon (driven by enhanced trade winds) may both contribute to increase Amazonian precipitation (Maslin et al., 2011) during the last glacial period and older cold substages.

East–west anti-phasing precipitation changes documented during the mid-Holocene are mostly restricted to NE Brazil and have a small influence on easternmost Amazon (Tapajós and Xingu) tributaries only (Cruz et al., 2009; Prado et al., 2013a, b). Because these tributaries supply very little sediment material to the Amazon River (Meade et al., 1985; Guyot et al., 2007), east–west anti-phasing rainfall changes will have negligible influence on our %-Andes records. Enhanced Amazonian precipitation during periods of high DJF insolation could induce high %-Andes values (Fig. 6) in two ways. (1) Increased precipitation stimulates vegetation growth, which favours stabilization of bars and floodplains and trapping of sediments in Amazon lowland tributaries (Tal and Paola, 2007). Such processes would reduce the sediment delivery by lowland rivers during high DJF insolation and lead to increased %-Andes values (via the relative decrease in lowland material). (2) Increased precipitation over Andean basins during high DJF insolation (in line with Andean speleothem and lake sediment records, see references above) would enhance soil formation in the Andes, physical erosion and transport of suspended sediments by Andean tributaries (Meade, 1994), resulting in high %-Andes values

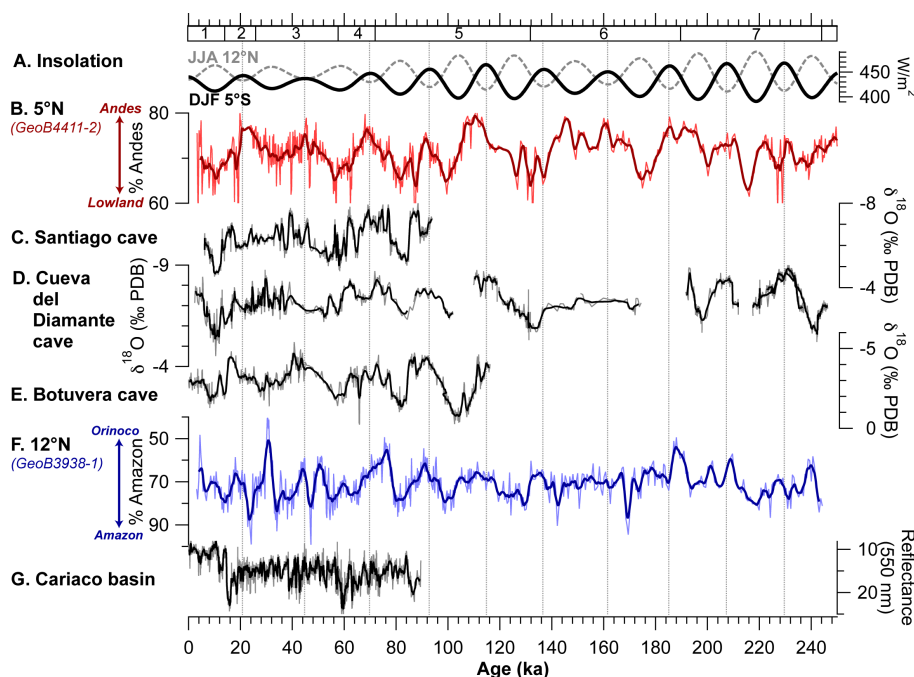


Fig. 8. Comparison with published records. (A) December-January-February (DJF, black line) and June-July-August (JJA, dashed grey line) insolation curves (Laskar et al., 2004). (B) %-Andes record from the core at 5° N (GeoB4411-2, same as in Fig. 6c). (C)–(E) Speleothem $\delta^{18}\text{O}$ records from Santiago cave (in C) (Mosblech et al., 2012), Cueva del Diamante cave (in D) (Cheng et al., 2013) and Botuverá cave (in E) (Cruz et al., 2005). (F) %-Amazon record from the core at 12° N (GeoB3938-1, same as in Fig. 6e but on a reversed scale). (G) Reflectance from ODP site 1002C from the Cariaco Basin (Peterson et al., 2000). Grey vertical dotted lines highlight DJF (JJA) insolation maxima (minima). See Fig. 1 for locations of published records. Marine isotope stages are indicated at the top of (A).

in marine sediments (Fig. 6). One may argue that enhanced Andean rainfall increased vegetation cover, which stabilized soils and limited the enhanced physical erosion in the Andes. However, pollen studies from the Ecuadorian (Colinvaux et al., 1997) and Colombian (Wille et al., 2001; van der Hammen and Hooghiemstra, 2003) Andes indicate that the transition between Andean forest and treeless “alpine” vegetation (paramo) shifted to lower altitudes during the LGM, in response to glacial cooling and steeper temperature gradients. By analogy, Andean arboreal vegetation cover was likely decreased during cold substages of the last 250 ka (i.e. periods of high DJF insolation, Fig. 6a–b), enhancing physical erosion and transport of sediments in the Andes. Finally, it is difficult to assess whether decreased lowland or increased Andean sediment supply dominates the high %-Andes signals recorded during periods of high DJF insolation. Large Andean precipitation changes indicated by Bolivian Altiplano lake sediments (Baker et al., 2001a, b; Fritz et al., 2007; Gosling et al., 2008; Hanselman et al., 2011) and western Amazonian speleothems (Fig. 8) (Mosblech et al., 2012; Cheng et al., 2013), as well as altitudinal shifts in the Andean forest belt (Colinvaux et al., 1997; Wille et al., 2001) suggest large past variations in sediment delivery by Andean tributaries (where most of modern terrigenous material originates, e.g. Meade et al., 1985; Guyot et al., 2007). However,

the lack of records documenting past lowland precipitation changes prevents firm conclusions.

We have assumed that the geochemical composition of endmembers remained constant through time, which is also a common assumption when interpreting elemental ratios (Zabel et al., 1999; Yarincik et al., 2000; Chiessi et al., 2010). However, the enhanced Amazonian rainfall (in particular in the Andes) indicated by speleothems (Mosblech et al., 2012; Cheng et al., 2013), lake sediments (Baker et al., 2001a, b; Fritz et al., 2007; Gosling et al., 2008; Hanselman et al., 2011) and model simulations (Cook and Vizy, 2006; Vizy and Cook, 2007) during periods of high DJF insolation could enhance chemical weathering and alter the composition of Andean and lowland endmembers. Currently, highly chemically weathered sediments from lowland regions exhibit high kaolinite content (Guyot et al., 2007) and are enriched in Al and Fe (Table S3 in the Supplement), while the slightly weathered material produced in the Andes is rich in illite (Guyot et al., 2007) and characterized by higher Si and K concentrations (Table S3 in the Supplement). Therefore, high %-Andes values indicate high (low) proportions of slightly (highly) weathered sediments that presently originate from Andean (lowland) regions. Enhanced rainfall in the Andes would lead to increased chemical weathering, bringing the composition of Andean material closer to that

of lowland sediments. Larger proportions of a more weathered Andean endmember (leading to even higher %-Andes values) would thus be required to represent the geochemical composition of lightly weathered terrigenous sediments observed during periods of high DJF insolation. Similarly, intensified chemical weathering due to enhanced rainfall in lowland regions would enrich lowland material in Al and Fe. Smaller proportions of a more weathered lowland endmember (leading again to even higher %-Andes values) are thus needed to explain the sedimentary elemental composition. The same reasoning is true for periods of low DJF insolation; lower %-Andes values are required to account for the reduced chemical weathering induced by lower Amazonian rainfall. Therefore, considering constant endmember compositions over time (i.e. neglecting the effect on the composition of source materials of past variations in chemical weathering induced by rainfall changes) leads to potential underestimation (overestimation) of %-Andes values during periods of high (low) DJF insolation, that is, to underestimate the amplitude of %-Andes variations during the last 250 ka. Our hypothesis that the %-Andes records indicate orbital-scale Amazonian rainfall variations in response to austral summer insolation changes will therefore still hold true, even if the composition of source material shifted over time.

The record at 9° N exhibits relatively high %-Andes values and weak precessional variations between ~ 15 and 60 ka (Fig. 6d). The reason why precessional changes are weak at 9° N but strong at 5° N during the last glacial period is not clear. Better resolved millennial-scale events due to higher sedimentation rates at 9° N (Fig. 3) could explain this feature. Nevertheless, Bolivian Altiplano lake sediments (e.g. Fritz et al., 2007; Gosling et al., 2008) and western Amazonian and southern Brazilian speleothems (Cruz et al., 2007; Mosblech et al., 2012; Cheng et al., 2013) also suggest weak precessional variability during past glacial intervals. Lake Titicaca sediment records exhibit strong glacial–interglacial variability over the last 370 ka. Specific sediment composition (e.g. high magnetic susceptibility, low total carbon, no carbonate) and increased sedimentation rates recorded during glacial periods likely reflect cold and wet conditions and increased erosion rates due to enhanced Andean precipitation and strong glacier expansions in the surrounding cordillera (Fritz et al., 2007; Gosling et al., 2008). Such increased erosion induced by glacier advances in the Andes could contribute to the relatively high %-Andes values observed at 9° N throughout the last glacial period (Fig. 6d). Weak glacial precessional variability indicated by speleothems is associated with relatively wet South American tropical conditions (Cruz et al., 2007; Mosblech et al., 2012; Cheng et al., 2013), which could also contribute to the relatively high glacial %-Andes values (Fig. 6d). This pattern has been attributed to glacial boundary conditions in the Northern Hemisphere whose effect on South American tropical rainfall overlaps precessional variations (Cruz et al., 2007). Large northern ice sheets and cold North Atlantic surface waters led to a

strong meridional sea surface temperature (SST) gradient that shifted the ITCZ southward (Chiang and Bitz, 2005). In addition, decreased SST in the equatorial western Atlantic (e.g. Jaeschke et al., 2007) enhanced the continental moisture transport by the NE trade winds, which resulted in intensified South American monsoonal precipitation during the last glacial period (Cruz et al., 2007). Unfortunately, our high-resolution record at 9° N is too short (Fig. 6d) to confirm if this pattern held during the penultimate glacial period.

5.4 Redistribution by surface ocean currents

The 12° N %-Amazon record exhibits significant precessional variations, as indicated by the filtered data (Fig. 6e) and spectral analysis (Fig. 7). Despite small offsets due to absolute age uncertainties, low %-Amazon values occur during most periods of high DJF insolation (Fig. 6e). Increased Amazon precipitation and sediment discharge (in particular from Andean regions) observed during intervals of high DJF insolation (Fig. 6c–d, see Sect. 5.3) were expected to increase the amount of Amazon sediments transported by the NBC, which in turn would produce high %-Amazon values at 12° N. The time series in Fig. 6e, however, exhibits the opposite pattern.

The %-Amazon tracer reflects relative changes in the amount of Amazon vs. Orinoco material. Is it possible that the observed %-Amazon variations at 12° N could be linked to climate changes in the Orinoco catchment? Presently, precipitation over the Orinoco Basin mostly falls during boreal summer (JJA), when the ITCZ has a northern position (Fig. 1b) (Grimm, 2011). By analogy with the modern situation, we expect reduced Orinoco precipitation during periods of low JJA insolation, when the ITCZ position is shifted to the south (Haug et al., 2001) in response to increased meridional temperature gradient in the Northern Hemisphere (e.g. Chiang and Bitz, 2005). This is in line with the latitudinal contraction of the South American rain belt proposed by Maslin et al. (2011) during the last glacial period. The resulting reduction in Orinoco precipitation and sediment discharge during intervals of low JJA insolation (i.e. high DJF insolation, Fig. 6a) would decrease the proportion of Orinoco material (i.e. increase %-Amazon values at the 12° N core site). A pattern opposite to the one expected for this scenario is observed (Fig. 6e), indicating that the %-Amazon record at 12° N is not solely driven by sediment inputs from the Amazon and Orinoco rivers.

We propose that surface ocean currents exert a strong influence on the %-Amazon record. During modern times, the NBC carries Amazon freshwater towards the Caribbean Sea mainly between January and June, while the NBC retroflexion deflects part of the Amazon plume eastward between July and December (Fig. 1) (e.g. Müller-Karger et al., 1988; Lentz, 1995). During intervals of high DJF (i.e. low JJA) insolation, which also correspond to cold substages of the last 250 ka (e.g. MIS 2, 4, 5.2, 5.4, 6.2, 6.4, Fig. 6a–b),

we suggest a seasonal intensification or prolongation in the duration of the NBC retroflection that deflected eastward freshwater and sediment input from the Amazon River. Such changes would explain the relative reduction in Amazon material (low %-Amazon values) recorded at 12° N during periods of high DJF insolation, despite the increased Amazon precipitation and sediment delivery recorded at 5 and 9° N (Fig. 6). This hypothesis is supported by the strengthening of the NBC retroflection and oceanward deflection of Amazon freshwater plume suggested during past cold substages and Heinrich events (Maslin, 1998; Rühlemann et al., 2001; Wilson et al., 2011). Larger northern ice sheets during cold substages (or iceberg discharge during Heinrich events) enhanced the Atlantic meridional SST gradient, which strengthened trade winds, shifted the ITCZ southward (Chiang and Bitz, 2005) and curtailed the cross-equatorial export of the NBC (Maslin, 1998). Intensified trade winds also favoured the accumulation of surface waters in the western equatorial Atlantic, creating a W–E pressure gradient (Rühlemann et al., 2001). This gradient strengthened the North Equatorial Counter Current and the NBC retroflection, that is, a more vigorous eastward flow of surface waters carrying freshwater and suspended particles delivered by the Amazon River (e.g. Maslin, 1998; Zabel et al., 1999; Rühlemann et al., 2001; Wilson et al., 2011). Because it is unlikely that surface-water currents discriminate between the Andean and lowland origin of suspended sediments delivered by the Amazon River, the %-Andes tracer is independent of sediment redistribution by surface ocean currents. However, the increased fraction of total terrigenous sediments recorded at 5° N during cold substages (Fig. 5a) may indicate enhanced delivery of detrital particles by the strengthened NBC retroflection (in addition to possible sea level effects, see Sect. 5.1), as has been observed in nearby sediment cores (Rühlemann et al., 2001).

Finally, the relationship between insolation and the %-Amazon record at 12° N is weaker during glacial times (170–140 ka and the last ~ 50 ka) than elsewhere (Fig. 6e), as already described for the core at 5° N (Fig. 6c, see Sect. 5.3). Such weak precessional signals are also observed during the last glacial period in the Cariaco Basin (Fig. 8), where millennial-scale variability dominates past changes in terrigenous material (Peterson et al., 2000). Large millennial-scale events that characterize the %-Amazon record during the last glacial period (between ~ 60 and 20 ka, Fig. 6e) most probably dominate over precessional variations.

6 Conclusions

We present high-resolution geochemical records from four marine sediment cores located between 5° and 12° N along the northern South American margin for the last 250 ka. By comparing the elemental composition of the sediments to major terrigenous sources, we show that detrital particles

derive solely from the Amazon River for cores at 5 and 9° N, while the site at 12° N receives a mixture of Amazon and Orinoco sediments. We have applied an endmember unmixing model to distinguish the relative proportions of Amazon Andean material (5 and 9° N) and of Amazon material (12° N) within the terrigenous fraction. We have considered processes (North African dust input, sea level changes, grain size sorting, reorganization in bottom-water currents) that potentially influence the derived %-Andes and %-Amazon tracers, and show that South American fluvial input is the main driver of %-Andes and %-Amazon variations at our core locations.

The %-Andes and %-Amazon records exhibit significant precessional variations. We suggest that high %-Andes values recorded during periods of high DJF insolation at 5 and 9° N reflect increased delivery of suspended sediments by Andean tributaries, resulting from enhanced Amazonian precipitation (in particular in the Andes). Observations from Bolivian Altiplano lake sediments and western Amazonian speleothems support our hypothesis. Increased Amazonian rainfall reflects the intensification of the South American monsoon in response to enhanced land–ocean thermal gradient and moisture transport during periods of high austral summer insolation.

In contrast, the record at 12° N exhibits low %-Amazon values during periods of high DJF insolation, that is, when enhanced Amazon precipitation and sediment discharge were expected to increase the amount of Amazon sediments carried northwestward by the NBC. We propose that reorganizations in surface ocean currents affect sediment transport and modulate the %-Amazon record at 12° N. During cold substages (periods of low JJA and high DJF insolation), we suggest that the seasonal intensification or prolongation in the duration of the NBC retroflection deflected eastward a large portion of the terrigenous input from the Amazon River, despite intensified Amazonian precipitation. The strengthening of the NBC retroflection may derive from a pile-up of surface waters in the western equatorial Atlantic in response to enhanced NE trade winds during cold substages (Rühlemann et al., 2001; Wilson et al., 2011).

Supplementary material related to this article is available online at <http://www.clim-past.net/10/843/2014/cp-10-843-2014-supplement.pdf>.

Acknowledgements. We thank M. Segl, B. Meyer-Schack, V. Lukies, M. Klann and S. Pape for technical support. We also thank Jennifer Kuhr and Janis Ahrens for the data acquired during their Master and Bachelor thesis, respectively. We acknowledge the Geoscience Department and the GeoB Core Repository at MARUM – University of Bremen for supplying sediment samples. This research used data acquired at the XRF Core Scanner Lab from MARUM – University of Bremen. The data reported in this paper are archived in Pangaea

(<http://doi.pangaea.de/10.1594/PANGAEA.831553>). This work was funded by the Deutsche Forschungsgemeinschaft (DFG) under the Special Priority Programme INTERDYNAMIC (EndLIG project). D. Heslop was funded by the Australian Research Council (grant DP110105419). C. M. Chiessi acknowledges financial support from FAPESP (grant 2012/17517-3). A. O. Sawakuchi thanks FAPESP for funding the project “Transport and Storage of Sediments in the Amazon rivers” (grant 2011/06609-1). Finally, we thank the reviewers (P. Baker and M. Maslin) and the editor (H. Fischer) for their constructive comments on the manuscript.

Edited by: H. Fischer

References

- Aalto, R., Dunne, T., and Guyot, J. L.: Geomorphic Controls on Andean Denudation Rates, *J. Geol.*, 114, 85–99, doi:10.1086/498101, 2006.
- Ahrens, J.: Klimavariationen im nördlichen Südamerika (Orinoco- und Amazonas-Becken) innerhalb der letzten 244 ka anhand von Elementverhältnissen, Bachelor thesis, Department of Geosciences, University of Bremen, Bremen, 2011.
- Antonov, J. I., Seidov, D., Boyer, T. P., Locarnini, R. A., Mishonov, A. V., Garcia, H. E., Baranova, O. K., Zweng, M. M., and Johnson, D. R.: World Ocean Atlas 2009, in: Volume 2: Salinity, edited by: Levitus, S., NOAA Atlas NESDIS 69, US Government Printing Office, Washington, D.C., 184 pp., 2010.
- Arz, H. W., Pätzold, J., and Wefer, G.: Correlated Millennial-Scale Changes in Surface Hydrography and Terrigenous Sediment Yield Inferred from Last-Glacial Marine Deposits off Northeastern Brazil, *Quaternary Res.*, 50, 157–166, doi:10.1006/qres.1998.1992, 1998.
- Arz, H. W., Pätzold, J., and Wefer, G.: Climatic changes during the last deglaciation recorded in sediment cores from the northeastern Brazilian Continental Margin, *Geo-Mar. Lett.*, 19, 209–218, 1999.
- Baker, P. A., Rigsby, C. A., Seltzer, G. O., Fritz, S. C., Lowenstein, T. K., Bacher, N. P., and Veliz, C.: Tropical climate changes at millennial and orbital timescales on the Bolivian Altiplano, *Nature*, 409, 698–701, doi:10.1038/35055524, 2001a.
- Baker, P. A., Seltzer, G. O., Fritz, S. C., Dunbar, R. B., Grove, M. J., Tapia, P. M., Cross, S. L., Rowe, H. D., and Broda, J. P.: The History of South American Tropical Precipitation for the Past 25,000 Years, *Science*, 291, 640–643, doi:10.1126/science.291.5504.640, 2001b.
- Bazin, L., Landais, A., Lemieux-Dudon, B., Toyé Mahamadou Kele, H., Veres, D., Parrenin, F., Martinerie, P., Ritz, C., Capron, E., Lipenkov, V., Loutre, M.-F., Raynaud, D., Vinther, B., Svensson, A., Rasmussen, S. O., Severi, M., Blunier, T., Leuenberger, M., Fischer, H., Masson-Delmotte, V., Chappellaz, J., and Wolff, E.: An optimized multi-proxy, multi-site Antarctic ice and gas orbital chronology (AICC2012): 120–800 ka, *Clim. Past*, 9, 1715–1731, doi:10.5194/cp-9-1715-2013, 2013.
- Behling, H.: South and southeast Brazilian grasslands during Late Quaternary times: a synthesis, *Palaeogeogr. Palaeoclimatol.*, 177, 19–27, doi:10.1016/S0031-0182(01)00349-2, 2002.
- Biscaye, P. E.: Mineralogy and Sedimentation of Recent Deep-Sea Clay in the Atlantic Ocean and Adjacent Seas and Oceans, *Geol. Soc. Am. Bull.*, 76, 803–832, 1965.
- Bleil, U. and cruise participants: Report and preliminary results of Meteor Cruise 38-2 Recife – Las Palmas, 04.03–14.04.1997, Berichte, Fachbereich Geowissenschaften, Universität Bremen, Bremen, 1998.
- Bleil, U. and Dobeneck, T.: Late Quaternary Terrigenous Sedimentation in the Western Equatorial Atlantic South American versus African Provenance Discriminated by Magnetic Mineral Analysis, in: *The South Atlantic in the Late Quaternary*, edited by: Wefer, G., Mulitza, S., and Ratmeyer, V., Springer, Berlin, Heidelberg, 213–236, 2004.
- Bloemsma, M. R., Zabel, M., Stuut, J. B. W., Tjallingii, R., Collins, J. A., and Weltje, G. J.: Modelling the joint variability of grain size and chemical composition in sediments, *Sediment. Geol.*, 280, 135–148, doi:10.1016/j.sedgeo.2012.04.009, 2012.
- Blum, M., Martin, J., Milliken, K., and Garvin, M.: Paleovalley systems: Insights from Quaternary analogs and experiments, *Earth-Sci. Rev.*, 116, 128–169, doi:10.1016/j.earscirev.2012.09.003, 2013.
- Bouchez, J., Gaillardet, J., France-Lanord, C., Maurice, L., and Dutra-Maia, P.: Grain size control of river suspended sediment geochemistry: Clues from Amazon River depth profiles, *Geochem. Geophys. Geosy.*, 12, Q03008, doi:10.1029/2010gc003380, 2011.
- Chappellaz, J., Blunier, T., Raynaud, D., Barnola, J. M., Schwander, J., and Stauffert, B.: Synchronous changes in atmospheric CH₄ and Greenland climate between 40 and 8 kyr BP, *Nature*, 366, 443–445, doi:10.1038/366443a0, 1993.
- Cheng, H., Sinha, A., Cruz, F. W., Wang, X., Edwards, R. L., d’Horta, F. M., Ribas, C. C., Vuille, M., Stott, L. D., and Auler, A. S.: Climate change patterns in Amazonia and biodiversity, *Nat. Commun.*, 4, 1411, doi:10.1038/ncomms2415, 2013.
- Chiang, J. and Bitz, C.: Influence of high latitude ice cover on the marine Intertropical Convergence Zone, *Clim. Dynam.*, 25, 477–496, doi:10.1007/s00382-005-0040-5, 2005.
- Chiessi, C. M., Mulitza, S., Pätzold, J., and Wefer, G.: How different proxies record precipitation variability over southeastern South America, *IOP Conf. Ser. Earth Environ. Sci.*, 9, 012007, doi:10.1088/1755-1315/9/1/012007, 2010.
- Colinvaux, P. A., Bush, M. B., Steinitz-Kannan, M., and Miller, M. C.: Glacial and Postglacial Pollen Records from the Ecuadorian Andes and Amazon, *Quaternary Res.*, 48, 69–78, doi:10.1006/qres.1997.1908, 1997.
- Collins, J. A., Govin, A., Mulitza, S., Heslop, D., Zabel, M., Hartmann, J., Röhl, U., and Wefer, G.: Abrupt shifts of the Sahara-Sahel boundary during Heinrich stadials, *Clim. Past*, 9, 1181–1191, doi:10.5194/cp-9-1181-2013, 2013.
- Cook, K. H. and Vizy, E. K.: South American climate during the Last Glacial Maximum: Delayed onset of the South American monsoon, *J. Geophys. Res.-Atmos.*, 111, D02110, doi:10.1029/2005jd005980, 2006.
- Cruz, F. W., Burns, S. J., Karmann, I., Sharp, W. D., Vuille, M., Cardoso, A. O., Ferrari, J. A., Silva Dias, P. L., and Viana, O.: Insolation-driven changes in atmospheric circulation over the past 116,000 years in subtropical Brazil, *Nature*, 434, 63–66, doi:10.1038/nature03365, 2005.

- Cruz, F. W., Burns, S. J., Jercinovic, M., Karmann, I., Sharp, W. D., and Vuille, M.: Evidence of rainfall variations in Southern Brazil from trace element ratios (Mg/Ca and Sr/Ca) in a Late Pleistocene stalagmite, *Geochim. Cosmochim. Acta*, 71, 2250–2263, doi:10.1016/j.gca.2007.02.005, 2007.
- Cruz, F. W., Vuille, M., Burns, S. J., Wang, X., Cheng, H., Werner, M., Lawrence Edwards, R., Karmann, I., Auler, A. S., and Nguyen, H.: Orbitally driven east-west antiphasing of South American precipitation, *Nat. Geosci.*, 2, 210–214, doi:10.1038/ngeo444, 2009.
- Curry, W. B. and Oppo, D. W.: Synchronous, high-frequency oscillations in tropical sea surface temperatures and North Atlantic Deep Water production during the Last Glacial Cycle, *Paleoceanography*, 12, 1–14, doi:10.1029/96pa02413, 1997.
- Davidson, E. A., de Araujo, A. C., Artaxo, P., Balch, J. K., Brown, I. F., Bustamante, M. M., Coe, M. T., DeFries, R. S., Keller, M., Longo, M., Munger, J. W., Schroeder, W., Soares-Filho, B. S., Souza, C. M., and Wofsy, S. C.: The Amazon basin in transition, *Nature*, 481, 321–328, doi:10.1038/nature10717, 2012.
- DeMaster, D. J., Knapp, G. B., and Nittrouer, C. A.: Biological uptake and accumulation of silica on the Amazon continental shelf, *Geochim. Cosmochim. Acta*, 47, 1713–1723, doi:10.1016/0016-7037(83)90021-2, 1983.
- Eisma, D., Van Der Gaast, S. J., Martin, J. M., and Thomas, A. J.: Suspended matter and bottom deposits of the Orinoco delta: Turbidity, mineralogy and elementary composition, *Neth. J. Sea Res.*, 12, 224–251, doi:10.1016/0077-7579(78)90007-8, 1978.
- Fischer, G. and cruise participants: Report and preliminary results of RV Meteor Cruise M34/4 Recife – Bridgetown, 19.03–15.04.1996, *Berichte, Fachbereich Geowissenschaften, Universität Bremen, Bremen*, 105 pp., 1996.
- Fischer, G. and cruise participants: Report and preliminary results of RV Meteor Cruise M49/4 Salvador da Bahia – Halifax, 04.04–05.05.2001, *Berichte, Fachbereich Geowissenschaften, Universität Bremen, Bremen*, 2002.
- Fritz, S. C., Baker, P. A., Seltzer, G. O., Ballantyne, A., Tapia, P., Cheng, H., and Edwards, R. L.: Quaternary glaciation and hydrologic variation in the South American tropics as reconstructed from the Lake Titicaca drilling project, *Quaternary Res.*, 68, 410–420, doi:10.1016/j.yqres.2007.07.008, 2007.
- Fritz, S. C., Baker, P. A., Ekdahl, E., Seltzer, G. O., and Stevens, L. R.: Millennial-scale climate variability during the Last Glacial period in the tropical Andes, *Quaternary Sci. Rev.*, 29, 1017–1024, doi:10.1016/j.quascirev.2010.01.001, 2010.
- Gerhardt, S. and Henrich, R.: Shell preservation of *Limacina inflata* (Pteropoda) in surface sediments from the Central and South Atlantic Ocean: a new proxy to determine the aragonite saturation state of water masses, *Deep-Sea Res. Pt. I*, 48, 2051–2071, doi:10.1016/S0967-0637(01)00005-X, 2001.
- Gerhardt, S., Groth, H., Rühlemann, C., and Henrich, R.: Aragonite preservation in late Quaternary sediment cores on the Brazilian Continental Slope: implications for intermediate water circulation, *Int. J. Earth Sci.*, 88, 607–618, doi:10.1007/s005310050291, 2000.
- Ghil, M., Allen, M. R., Dettinger, M. D., Ide, K., Kondrashov, D., Mann, M. E., Robertson, A. W., Saunders, A., Tian, Y., Varadi, F., and Yiou, P.: Advanced spectral methods for climatic time series, *Rev. Geophys.*, 40, 1003, doi:10.1029/2000rg000092, 2002.
- Gosling, W. D., Bush, M. B., Hanselman, J. A., and Chepstow-Lusty, A.: Glacial-interglacial changes in moisture balance and the impact on vegetation in the southern hemisphere tropical Andes (Bolivia/Peru), *Palaeogeography, Palaeoclimatology, Palaeoecology*, 259, 35–50, doi:10.1016/j.palaeo.2007.02.050, 2008.
- Govin, A., Holzwarth, U., Heslop, D., Ford Keeling, L., Zabel, M., Mulitza, S., Collins, J. A., and Chiessi, C. M.: Distribution of major elements in Atlantic surface sediments (36° N–49° S): Impprint of terrigenous input and continental weathering, *Geochem. Geophys. Geosy.*, 13, Q01013, doi:10.1029/2011gc003785, 2012.
- Grimm, A. M.: Interannual climate variability in South America: impacts on seasonal precipitation, extreme events, and possible effects of climate change, *Stoch. Environ. Res. Risk. Assess.*, 25, 537–554, doi:10.1007/s00477-010-0420-1, 2011.
- Grimm, A. M., Vera, C. S., and Mechoso, C. R.: 15. The South American monsoon system, in: *The global monsoon system: research and forecast*, edited by: Chang, C. P., Wang, B., and Lau, N.-C. G., World Meteorological Organization, Geneva, Switzerland, 2005.
- Guyot, J. L., Jouanneau, J. M., Soares, L., Boaventura, G. R., Maillet, N., and Lagane, C.: Clay mineral composition of river sediments in the Amazon Basin, *Catena*, 71, 340–356, doi:10.1016/j.catena.2007.02.002, 2007.
- Hanselman, J. A., Bush, M. B., Gosling, W. D., Collins, A., Knox, C., Baker, P. A., and Fritz, S. C.: A 370,000-year record of vegetation and fire history around Lake Titicaca (Bolivia/Peru), *Palaeogeogr. Palaeoclimatol.*, 305, 201–214, doi:10.1016/j.palaeo.2011.03.002, 2011.
- Harris, S. E. and Mix, A. C.: Pleistocene Precipitation Balance in the Amazon Basin Recorded in Deep Sea Sediments, *Quaternary Res.*, 51, 14–26, doi:10.1006/qres.1998.2008, 1999.
- Haug, G. H., Hughen, K. A., Sigman, D. M., Peterson, L. C., and Rohl, U.: Southward Migration of the Intertropical Convergence Zone Through the Holocene, *Science*, 293, 1304–1308, 2001.
- Höll, C., Karwath, B., Rühlemann, C., Zonneveld, K. A. F., and Willems, H.: Palaeoenvironmental information gained from calcareous dinoflagellates: the late Quaternary eastern and western tropical Atlantic Ocean in comparison, *Palaeogeogr. Palaeoclimatol.*, 146, 147–164, doi:10.1016/S0031-0182(98)00141-2, 1999.
- Hörner, T.: Relation between Amazonian precipitation, insolation and ocean circulation during the last 250 kyr, Master thesis, Department of Geosciences, University of Bremen, Bremen, 2012.
- Hu, C., Montgomery, E. T., Schmitt, R. W., and Muller-Karger, F. E.: The dispersal of the Amazon and Orinoco River water in the tropical Atlantic and Caribbean Sea: Observation from space and S-PALACE floats, *Deep-Sea Res. Pt. II*, 51, 1151–1171, doi:10.1016/j.dsr2.2004.04.001, 2004.
- Huber, C., Leuenberger, M., Spahni, R., Fluckiger, J., Schwander, J., Stocker, T. F., Johnsen, S., Landais, A., and Jouzel, J.: Isotope calibrated Greenland temperature record over Marine Isotope Stage 3 and its relation to CH₄, *Earth Planet. Sc. Lett.*, 243, 504–519, 2006.
- Jaeschke, A., Rühlemann, C., Arz, H., Heil, G., and Lohmann, G.: Coupling of millennial-scale changes in sea surface temperature and precipitation off northeastern Brazil with high-latitude climate shifts during the last glacial period, *Paleoceanography*, 22, PA4206, doi:10.1029/2006pa001391, 2007.

- Kanner, L. C., Burns, S. J., Cheng, H., and Edwards, R. L.: High-Latitude Forcing of the South American Summer Monsoon During the Last Glacial, *Science*, 335, 570–573, doi:10.1126/science.1213397, 2012.
- Kohfeld, K. E. and Harrison, S. P.: DIRTMAP: the geological record of dust, *Earth-Sci. Rev.*, 54, 81–114, doi:10.1016/S0012-8252(01)00042-3, 2001.
- Kuhr, J.: Spätquartäre Niederschlagsveränderungen im Amazonasbecken: Einfluß von Sonneneinstrahlung und Ozeanzirkulation, Master thesis, Department of Geosciences, University of Bremen, Bremen, 2011.
- Laskar, J., Robutel, P., Joutel, F., Gastineau, M., Correia, A. C. M., and Levrard, B.: A long-term numerical solution for the insolation quantities of the Earth, *Astron. Astrophys.*, 428, 261–285, 2004.
- Ledru, M.-P., Mourguiart, P., and Riccomini, C.: Related changes in biodiversity, insolation and climate in the Atlantic rainforest since the last interglacial, *Palaeogeography, Palaeoclimatology, Palaeoecology*, 271, 140–152, doi:10.1016/j.palaeo.2008.10.008, 2009.
- Lentz, S. J.: Seasonal variations in the horizontal structure of the Amazon Plume inferred from historical hydrographic data, *J. Geophys. Res.-Oceans*, 100, 2391–2400, doi:10.1029/94jc01847, 1995.
- Lewis, S. L., Brando, P. M., Phillips, O. L., van der Heijden, G. M. F., and Nepstad, D.: The 2010 Amazon Drought, *Science*, 331, 554–554, doi:10.1126/science.1200807, 2011.
- Lisiecki, L. E. and Raymo, M. E.: A Pliocene-Pleistocene stack of 57 globally distributed benthic $\delta^{18}\text{O}$ records, *Paleoceanography*, 20, PA1003, doi:10.1029/2004pa001071, 2005.
- Loulergue, L., Schilt, A., Spahni, R., Masson-Delmotte, V., Blunier, T., Lemieux, B., Barnola, J. M., Raynaud, D., Stocker, T. F., and Chappellaz, J.: Orbital and millennial-scale features of atmospheric CH_4 over the past 800,000 years, *Nature*, 453, 383–386, 2008.
- Mahowald, N. M., Muhs, D. R., Levis, S., Rasch, P. J., Yoshioka, M., Zender, C. S., and Luo, C.: Change in atmospheric mineral aerosols in response to climate: Last glacial period, preindustrial, modern, and doubled carbon dioxide climates, *J. Geophys. Res.*, 111, D10202, doi:10.1029/2005jd006653, 2006.
- Malhi, Y., Roberts, J. T., Betts, R. A., Killeen, T. J., Li, W., and Nobre, C. A.: Climate Change, Deforestation, and the Fate of the Amazon, *Science*, 319, 169–172, doi:10.1126/science.1146961, 2008.
- Marengo, J. A., Nobre, C. A., Tomasella, J., Oyama, M. D., Sampaio de Oliveira, G., de Oliveira, R., Camargo, H., Alves, L. M., and Brown, I. F.: The Drought of Amazonia in 2005, *J. Climate*, 21, 495–516, doi:10.1175/2007jcli1600.1, 2008.
- Marengo, J. A., Tomasella, J., Soares, W., Alves, L., and Nobre, C.: Extreme climatic events in the Amazon basin, *Theor. Appl. Climatol.*, 107, 73–85, doi:10.1007/s00704-011-0465-1, 2012.
- Masek, J. G., Isacks, B. L., Gubbels, T. L., and Fielding, E. J.: Erosion and tectonics at the margins of continental plateaus, *J. Geophys. Res.-Solid*, 99, 13941–13956, doi:10.1029/94jb00461, 1994.
- Maslin, M.: Equatorial western Atlantic Ocean circulation changes linked to the Heinrich events: deep-sea sediment evidence from the Amazon Fan, Geological Society, London, Special Publications, 131, 111–127, doi:10.1144/gsl.sp.1998.131.01.09, 1998.
- Maslin, M., Knutz, P. C., and Ramsay, T.: Millennial-scale sea-level control on avulsion events on the Amazon Fan, *Quaternary Sci. Rev.*, 25, 3338–3345, doi:10.1016/j.quascirev.2006.10.012, 2006.
- Maslin, M. A., Ettwein, V. J., Wilson, K. E., Guilderson, T. P., Burns, S. J., and Leng, M. J.: Dynamic boundary-monsoon intensity hypothesis: evidence from the deglacial Amazon River discharge record, *Quaternary Sci. Rev.*, 30, 3823–3833, doi:10.1016/j.quascirev.2011.10.007, 2011.
- Meade, R. H.: Suspended sediments of the modern Amazon and Orinoco rivers, *Quatern. Int.*, 21, 29–39, doi:10.1016/1040-6182(94)90019-1, 1994.
- Meade, R. H.: River-sediment inputs to major deltas, in: *Sea-level Rise and Coastal Subsidence*, edited by: Milliman, J. D. and Haq, B. U., Kluwer Academic Publishers, Dordrecht, the Netherlands, 63–85, 1996.
- Meade, R. H., Dunne, T., Richey, J. E., De M. Santos, U., and Salati, E.: Storage and Remobilization of Suspended Sediment in the Lower Amazon River of Brazil, *Science*, 228, 488–490, doi:10.1126/science.228.4698.488, 1985.
- Meade, R. H., Weibezahn, F. H., Lewis, W. N., and Pérez-Hernández, D.: Suspended-sediment budget for the Orinoco River, in: *El Río Orinoco como Ecosistema*, edited by: Weibezahn, F. H., Alvarez, H., and Lewis, J. W. M., Impresos Rubel, Caracas, Venezuela, 55–79, 1990.
- Milliman, J. D., Summerhayes, C. P., and Barretto, H. T.: Quaternary Sedimentation on the Amazon Continental Margin: A Model, *Geol. Soc. Am. Bull.*, 86, 610–614, doi:10.1130/0016-7606(1975)86<610:qsoac>2.0.co;2, 1975.
- Moore, B. R. and Dennen, W. H.: A geochemical trend in silicon-aluminum-iron ratios and the classification of clastic sediments, *J. Sediment. Res.*, 40, 1147–1152, doi:10.1306/74D72153-2B21-11D7-8648000102C1865D, 1970.
- Mosblech, N. A. S., Bush, M. B., Gosling, W. D., Hodell, D., Thomas, L., van Calsteren, P., Correa-Metrio, A., Valencia, B. G., Curtis, J., and van Woesik, R.: North Atlantic forcing of Amazonian precipitation during the last ice age, *Nat. Geosci.*, 5, 817–820, doi:10.1038/ngeo1588, 2012.
- Mulitza, S., Prange, M., Stuut, J.-B. W., Zabel, M., von Dobe-neck, T., Itambi, A. C., Nizou, J., Schulz, M., and Wefer, G.: Sahel megadroughts triggered by glacial slowdowns of Atlantic meridional overturning, *Paleoceanography*, 23, PA4206, doi:10.1029/2008pa001637, 2008.
- Mulitza, S., Heslop, D., Pittauerova, D., Fischer, H. W., Meyer, I., Stuut, J.-B. W., Zabel, M., Mollenhauer, G., Collins, J. A., Kuhnert, H., and Schulz, M.: Increase in African dust flux at the onset of commercial agriculture in the Sahel region, *Nature*, 466, 226–228, doi:10.1038/nature09213, 2010.
- Müller-Karger, F. E., McClain, C. R., and Richardson, P. L.: The dispersal of the Amazon's water, *Nature*, 333, 56–59, doi:10.1038/333056a0, 1988.
- Müller-Karger, F. E., McClain, C. R., Fisher, T. R., Esaias, W. E., and Varela, R.: Pigment distribution in the Caribbean sea: Observations from space, *Prog. Oceanogr.*, 23, 23–64, doi:10.1016/0079-6611(89)90024-4, 1989.
- Nicholas, A.: Morphodynamic diversity of the world's largest rivers, *Geology*, 41, 475–478, doi:10.1130/g34016.1, 2013.

- Nobre, C. A. and Borma, L. D. S.: 'Tipping points' for the Amazon forest, *Curr. Opin. Environ. Sustain.*, 1, 28–36, doi:10.1016/j.cosust.2009.07.003, 2009.
- Peterson, L. C., Haug, G. H., Hughen, K. A., and Röhl, U.: Rapid Changes in the Hydrologic Cycle of the Tropical Atlantic During the Last Glacial, *Science*, 290, 1947–1951, doi:10.1126/science.290.5498.1947, 2000.
- Petschick, R., Kuhn, G., and Gingele, F.: Clay mineral distribution in surface sediments of the South Atlantic: sources, transport, and relation to oceanography, *Mar. Geol.*, 130, 203–229, doi:10.1016/0025-3227(95)00148-4, 1996.
- Peucker-Ehrenbrink, B.: Land2Sea database of river drainage basin sizes, annual water discharges, and suspended sediment fluxes, *Geochem. Geophys. Geosy.*, 10, Q06014, doi:10.1029/2008gc002356, 2009.
- Posamentier, H. W., Jervey, M. T., and Vail, P. R.: Eustatic controls on clastic deposition I – conceptual framework, in: *Sea-Level Changes: An Integrated Approach*, edited by: Wilgus, C. K., Hastings, B. S., Kendall, C. G. C., Posamentier, H. W., Ross, C. A., and Van Wagoner, J. C., SEPM Special Publication 42, Tulsa, Oklahoma, USA, 109–124, 1988.
- Prado, L. F., Wainer, I., and Chiessi, C. M.: Mid-Holocene PMP3/CMIP5 model results: Intercomparison for the South American Monsoon System, *Holocene*, 23, 1915–1920, doi:10.1177/0959683613505336, 2013a.
- Prado, L. F., Wainer, I., Chiessi, C. M., Ledru, M.-P., and Turcq, B.: A mid-Holocene climate reconstruction for eastern South America, *Clim. Past*, 9, 2117–2133, doi:10.5194/cp-9-2117-2013, 2013b.
- Rühlemann, C., Müller, P. J., and Schneider, R. R.: Organic Carbon and Carbonate as Paleoproductivity Proxies: Examples from High and Low Productivity Areas of the Tropical Atlantic, in: *Use of Proxies in Paleoceanography*, edited by: Fischer, G. and Wefer, G., Springer, Berlin, Heidelberg, 315–344, 1999.
- Rühlemann, C., Diekmann, B., Mulitza, S., and Frank, M.: Late Quaternary changes of western equatorial Atlantic surface circulation and Amazon lowland climate recorded in Ceará Rise deep-sea sediments, *Paleoceanography*, 16, 293–305, doi:10.1029/1999pa000474, 2001.
- Satyamurty, P., da Costa, C. P. W., Manzi, A. O., and Candido, L. A.: A quick look at the 2012 record flood in the Amazon Basin, *Geophys. Res. Lett.*, 40, 1396–1401, doi:10.1002/grl.50245, 2013.
- Schlünz, B., Schneider, R. R., Müller, P. J., and Wefer, G.: Late Quaternary organic carbon accumulation south of Barbados: influence of the Orinoco and Amazon rivers?, *Deep-Sea Res. Pt. I*, 47, 1101–1124, doi:10.1016/S0967-0637(99)00076-X, 2000.
- Schütz, L. and Rahn, K. A.: Trace-element concentrations in erodible soils, *Atmos. Environ.*, 16, 171–176, doi:10.1016/0004-6981(82)90324-9, 1982.
- Shackleton, N. J. and Opdyke, N. D.: Oxygen isotope and palaeomagnetic stratigraphy of Equatorial Pacific core V28-238: Oxygen isotope temperatures and ice volumes on a 105 year and 106 year scale, *Quaternary Res.*, 3, 39–55, doi:10.1016/0033-5894(73)90052-5, 1973.
- Shackleton, N. J., Hall, M. A., and Boersma, A.: 15. Oxygen and carbon isotope data from Leg 74 foraminifers, in: *Initial reports of the Deep Sea Drilling Project covering Leg 74 of the cruises of the drilling vessel Glomar Challenger, Cape Town, South Africa, to Walvis Bay, South Africa, June to July, 1980*, edited by: Moore Jr., T. C., Rabinowitz, P. D., Boersma, A., Borella, P. E., Chave, A. D., Duee, G., Fuetterer, D. K., Jiang, M.-J., Kleinert, K., Lever, A., Manivit, H., O'Connell, S., Richardson, S. H., Shackleton, N. J., Blakeslee, J. H., and Lee, M., Texas A & M University, Ocean Drilling Program, College Station, Texas, 599–612, 1984.
- Shackleton, N. J., Hall, M. A., and Vincent, E.: Phase relationships between millennial-scale events 64,000–24,000 years ago, *Paleoceanography*, 15, 565–569, 2000.
- Shackleton, N. J., Chapman, M. R., Sanchez-Goni, M. F., Pailler, D., and Lancelot, Y.: The classic Marine Isotope Substage 5e, *Quaternary Res.*, 58, 14–16, 2002.
- Sioli, H.: The Amazon and its main affluents: Hydrography, morphology of the river courses, and river types, in: *The Amazon, Monographiae Biologicae*, edited by: Sioli, H., Springer, Netherlands, 127–165, 1984.
- Sylvestre, F.: Moisture Pattern During the Last Glacial Maximum in South America, in: *Past Climate Variability in South America and Surrounding Regions*, edited by: Vimeux, F., Sylvestre, F., and Khodri, M., *Developments in Paleoenvironmental Research*, Springer, Netherlands, 3–27, 2009.
- Tal, M. and Paola, C.: Dynamic single-thread channels maintained by the interaction of flow and vegetation, *Geology*, 35, 347–350, doi:10.1130/g23260a.1, 2007.
- van der Hammen, T. and Hooghiemstra, H.: Interglacial-glacial Fuquene-3 pollen record from Colombia: an Eemian to Holocene climate record, *Global Planet. Change*, 36, 181–199, doi:10.1016/S0921-8181(02)00184-4, 2003.
- Vera, C., Higgins, W., Amador, J., Ambrizzi, T., Garreaud, R., Gochis, D., Gutzler, D., Lettenmaier, D., Marengo, J., Mechoso, C. R., Nogues-Paegle, J., Dias, P. L. S., and Zhang, C.: Toward a Unified View of the American Monsoon Systems, *J. Climate*, 19, 4977–5000, doi:10.1175/jcli3896.1, 2006.
- Veres, D., Bazin, L., Landais, A., Toyé Mahamadou Kele, H., Lemieux-Dudon, B., Parrenin, F., Martinerie, P., Blayo, E., Blunier, T., Capron, E., Chappellaz, J., Rasmussen, S. O., Severi, M., Svensson, A., Vinther, B., and Wolff, E. W.: The Antarctic ice core chronology (AICC2012): an optimized multi-parameter and multi-site dating approach for the last 120 thousand years, *Clim. Past*, 9, 1733–1748, doi:10.5194/cp-9-1733-2013, 2013.
- Vizy, E. K. and Cook, K. H.: Relationship between Amazon and high Andes rainfall, *J. Geophys. Res.-Atmos.*, 112, D07107, doi:10.1029/2006jd007980, 2007.
- Volbers, A. N. A. and Henrich, R.: Calcium carbonate corrosiveness in the South Atlantic during the Last Glacial Maximum as inferred from changes in the preservation of Globigerina bulloides: a proxy to determine deep-water circulation patterns?, *Mar. Geol.*, 204, 43–57, 2004.
- Wang, X., Auler, A. S., Edwards, R. L., Cheng, H., Cristalli, P. S., Smart, P. L., Richards, D. A., and Shen, C.-C.: Wet periods in northeastern Brazil over the past 210 kyr linked to distant climate anomalies, *Nature*, 432, 740–743, doi:10.1038/nature03067, 2004.
- Warne, A. G., Meade, R. H., White, W. A., Guevara, E. H., Gibeaut, J., Smyth, R. C., Aslan, A., and Tremblay, T.: Regional controls on geomorphology, hydrology, and ecosystem integrity in the Orinoco Delta, Venezuela, *Geomorphology*, 44, 273–307, doi:10.1016/S0169-555X(01)00179-9, 2002.

- Weltje, G. J. and Tjallingii, R.: Calibration of XRF core scanners for quantitative geochemical logging of sediment cores: Theory and application, *Earth Planet. Sc. Lett.*, 274, 423–438, doi:10.1016/j.epsl.2008.07.054, 2008.
- Wille, M., Hooghiemstra, H., Behling, H., van der Borg, K., and Negret, A. J.: Environmental change in the Colombian subandean forest belt from 8 pollen records: the last 50 kyr, *Veg. Hist. Archaeobot.*, 10, 61–77, doi:10.1007/pl00006921, 2001.
- Wilson, K. E., Maslin, M. A., and Burns, S. J.: Evidence for a prolonged retroflexion of the North Brazil Current during glacial stages, *Palaeogeography, Palaeoclimatology, Palaeoecology*, 301, 86–96, doi:10.1016/j.palaeo.2011.01.003, 2011.
- Yarincik, K. M., Murray, R. W., and Peterson, L. C.: Climatically Sensitive Eolian and Hemipelagic Deposition in the Cariaco Basin, Venezuela, Over the Past 578,000 Years: Results From Al/Ti and K/Al, *Paleoceanography*, 15, 210–228, doi:10.1029/1999pa900048, 2000.
- Zabel, M., Bickert, T., Dittert, L., and Haese, R. R.: Significance of the Sedimentary Al/Ti Ratio as an Indicator for Variations in the Circulation Patterns of the Equatorial North Atlantic, *Paleoceanography*, 14, 789–799, doi:10.1029/1999pa900027, 1999.